Enhanced validation data

Anti-PD-L1 recombinant antibody - ab237726

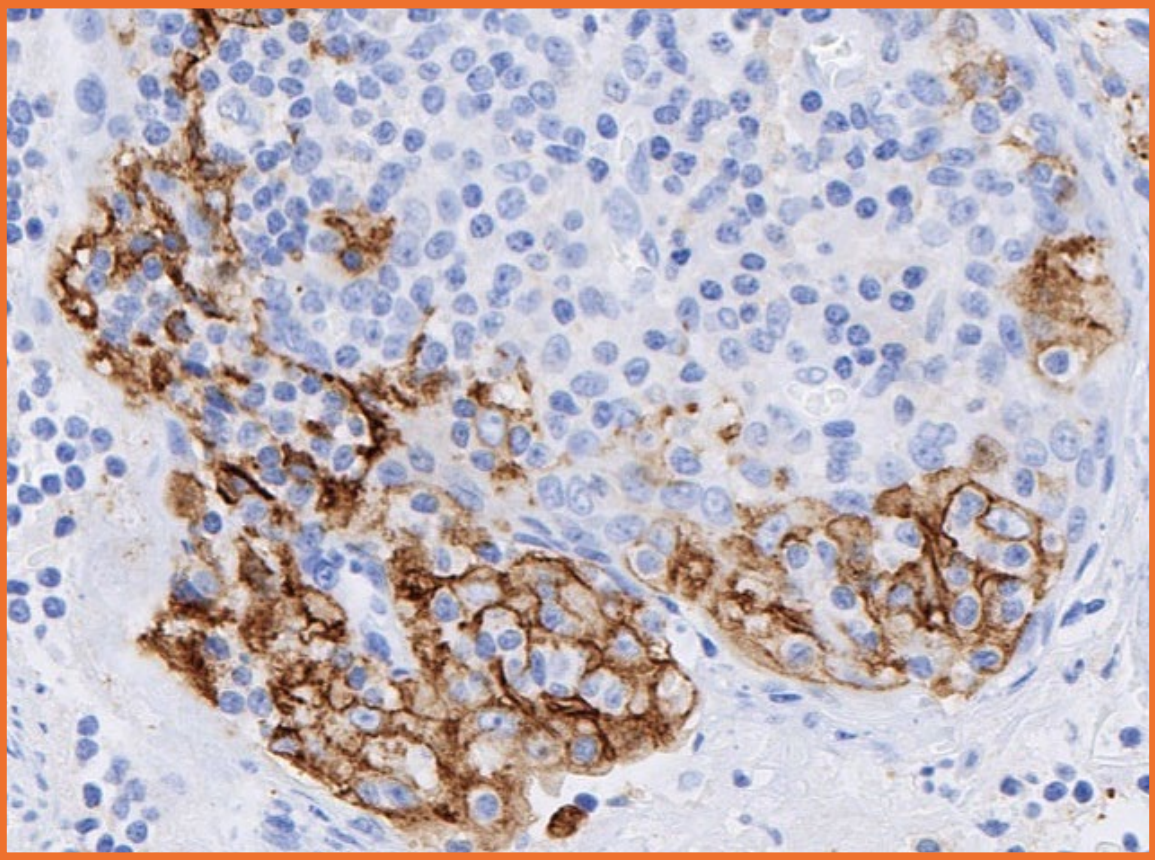

PD-L1 expression in human tonsil

progress happens together

abcam

AB0589_v1.0_120425

Enhanced validation of Anti-PD-L1 antibody [CAL10] – ab237726

Enhanced validation designed for your needs

We understand the challenge of finding the right antibody clone – highly specific and sensitive to your intended target – at early selection stages of your development program. To de-risk this clone selection process for you, we generated enhanced validation data for our best recombinant antibody clones to some of the most promising targets.

Our enhanced validation gives you an extra level of confidence in an antibody clone

— Provides additional data on the specificity and sensitivity of our recombinant antibodies in immunohistochemistry (IHC) and other relevant techniques

— Carried out in a custom manner, specific both to the target and the relevant research and clinical settings

— Builds upon our high-quality standard validation

Our framework for enhanced validation

— Our enhanced validation focuses on generating detailed IHC expression profiles for promising oncology targets in selected formalin-fixed paraffin-embedded (FFPE) human normal tissues and cancer tissue microarrays (TMAs).

— In this study, we demonstrate the sensitivity and specificity of Anti-PD-L1 antibody (ab237726) in IHC in selected tissues and TMAs using a BOND™ RX Research Stainer (Leica®) and DISCOVERY ULTRA system (Roche Diagnostics).

— A quantitative H-score analysis of PD-L1 expression was performed using the artificial intelligence (AI)-driven digital image analysis software Visiopharm® (Visiopharm A/S).

AB0589_v1.0_120425

Target overview

HGNC symbol
CD274

Approved name
CD274 molecule

Chromosomal location
9p24.1

Function

PD-L1 has several important functions in cellular processes including regulating transcription[1], driving cell cycle progression[2], preserving chromatin architecture[3], organizing super-enhancers[4], and facilitating the DNA damage response[5].

Tissue specificity

PD-L1 is found in several normal tissues, such as the placenta, colon, skin, tonsils, and spleen[6]. Its expression is markedly increased in various cancers, including gastric, nasopharyngeal, liver, and testicular tumors[7].

Cellular localization

Cell membrane

Database links

Entrez Gene: 29126
OMIM®: 605402
Uniprot: Q9NZQ7

Materials and methods

Human tissues were selected based on the target's expression and its current relevance to ongoing research and clinical trials. Gene expression was further analyzed for oncology targets in cBioPortal for Cancer Genomics using the Cancer Genome Atlas (TCGA) PanCancer Atlas datasets[8-11].

Tissue microarray (TMA)	Cores	Cases	Normal/ Benign cases	Cancer cases	Source (#catalog number)
Multi-normal [(a)]	15	15	15	0	In-house TMA
Multi-cancer [(b)]	35	35	1	34	In-house TMA
Breast cancer	96	48	0	48	Pantomics (#BRC964)
Lung cancer	102	102	5	97	Pantomics (#LUC1021)
Bladder cancer	102	102	5	97	Pantomics (#BLC1021)

Table 1. List of human TMAs used in the enhanced validation. All tissues were sourced from Abcam-approved tissue suppliers.

a) The multi-normal TMA consists of the following tissues from a single donor: colon, cerebrum, tonsil, stomach, testis, prostate, lung, skeletal muscle, heart, skin, spleen, pancreas, kidney, placenta and liver.

b) The multi-cancer TMA consists of the following tissues from two donors: seminoma, prostate adenocarcinoma, bladder carcinoma, renal cell carcinoma, melanoma, stomach adenocarcinoma, pancreatic adenocarcinoma, hepatocellular carcinoma, ovaria carcinoma, cervical cancer, head and neck carcinoma and endometrial cancer. The following tissues were from single donors: lung (squamous cell carcinoma (SCLC) and non-squamous cell carcinoma (NSCLC)), colon (adenocarcinoma and invasive adenocarcinoma), breast (ductal carcinoma and invasive lobular carcinoma), B cell lymphoma, T cell lymphoma, gliomas (grade II and IV) and placenta.

Step	Reagents	Method
Deparaffinization	DISCOVERY Wash (RUO)	Standard
Cell conditioning	ULTRA Cell Conditioning Solution (ULTRA CC1)	32 min, 100 °C
Pre-primary peroxidase inhibitor	OptiView Peroxidase Inhibitor	4 min
Primary antibody	Anti-PD-L1 antibody [CAL10] – ab237726 diluted in Discovery antibody diluent (#760-108) final concentration of 2.0 µg/mL	16 min, 37 °C
Counterstain	Hematoxylin II	8 min
Post counterstain	Bluing Reagent	4 min

Table 2. IHC staining protocol on the DISCOVERY ULTRA (Roche Diagnostics) instrument. Staining was performed using standard conditions with OptiView DAB IHC Detection kit (#760-700).

Enhanced validation data

Step	Reagents	Method
Dewax	Bond™ dewax solution (AR922), alcohol, BOND wash solution (AR9590)	Dewax
Antigen retrieval	Bond™ epitope retrieval ER2 solution (AR9640)	HIER with ER2 (pH 9.0), 20 min, 100°C

Step	Reagents	Number of washes	Time (minutes)
Peroxide block	3-4% (v/v) Hydrogen peroxide	-	5
Wash	Bond™ wash solution	3x	0
Primary antibody	Anti-PD-L1 antibody [CAL10] – ab237726 diluted in Bond™ primary antibody diluent (#AR9352) to final concentration of 0.75 µg/mL	-	15
Wash	Bond™ wash solution	4x	0
Secondary antibody	Bond™ polymer refine detection (DS9800)	-	8
Wash	Bond™ wash solution	2x	4
	Deionized water	1x	0
Visualization	Mixed DAB refine (DS9800)	1x	0
	Mixed DAB refine (DS9800)	-	10
Wash	Deionized water	3x	0
Counterstain	Hematoxylin (DS9800)	-	5
Wash	Deionized water	1x	0
	Bond™ wash solution	1x	0
	Deionized water	1x	0

Table 3. IHC staining protocol on BOND™ RX Research Stainer (Leica®). The protocol used is the same as the default IHC protocol F on BOND™ RX Research Stainer (Leica®), apart from the standard post-primary step, which has been excluded from our protocol. All steps were performed at room temperature.

H-score analysis

A quantitative H-score analysis of PD-L1 expression was performed using the artificial intelligence (AI)-driven digital image analysis software Visiopharm® (Version: 2023.09). TMA slides were de-arrayed and the tissue within each core was detected. Tissue detection, artefact exclusion and segmentation were performed using models with DeepLabv3+ architecture.

Total cell numbers for each core were counted using a trained AI model with U-Net architecture. Using the cell analysis data and thresholds, cell membrane H-scores of the tumor compartment in the TMAs were calculated in Visiopharm® and the graphical representation was generated using GraphPad Prism 10.

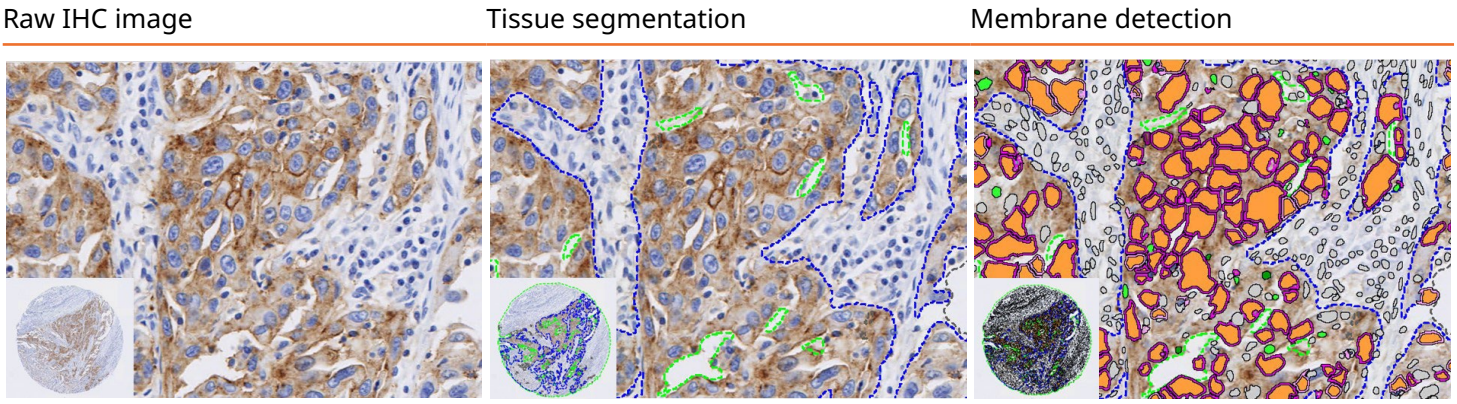

Figure 1. Visiopharm® tissue segmentation and membrane detection: Raw IHC images were subjected to total cell detection to determine staining intensity. There are four intensity scores shown in the example image here: grey (0), pink (1+), magenta (2+) and purple (3+). Areas in orange are irrelevant to these analyses.

IHC staining	Corresponding intensity score	Visiopharm® intensity threshold
Negative	0	> 255
Weak	1+	< 255
Moderate	2+	< 190
Strong	3+	< 160

Table 4. Intensity scoring and thresholds for H-score analysis. The H-score captures both the IHC staining intensity and the percentage of stained cells at each intensity level. It was calculated using the formula H-score = [(0x % of negative cells) + (1x % of weak stained cells) + (2x % of moderate stained cells) + (3x % of strong stained cells), giving an analytical range from 0 to 300.

PD-L1 expression in multi-normal TMA (BOND™ RX)

Below are the representative images of selected tissues from the multi-normal TMA. PD-L1 expression was detected in the placenta, spleen and tonsil; no expression was observed in the skin, testis, heart, prostate, liver, colon, stomach or skeletal muscle.

Placenta

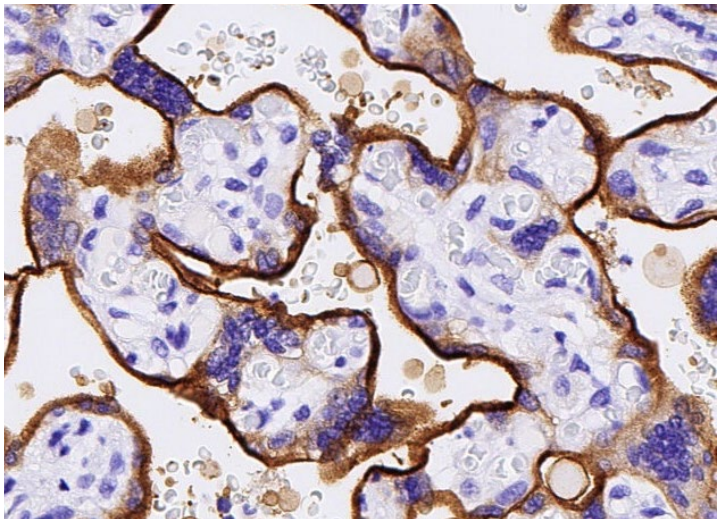

Skin

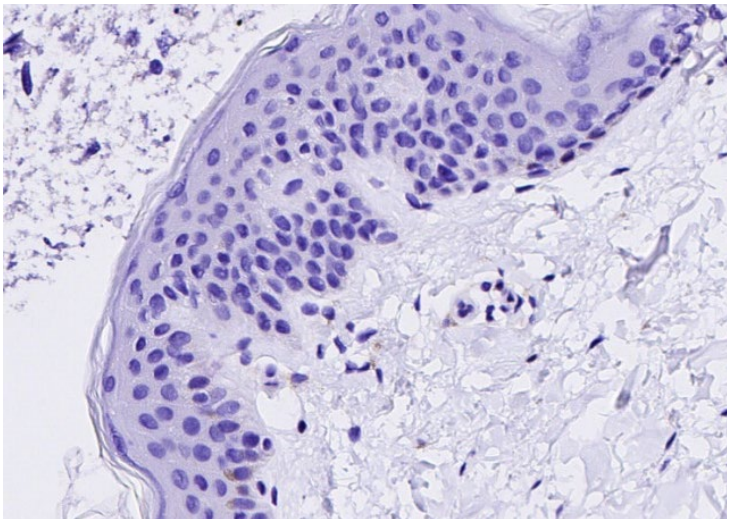

Spleen

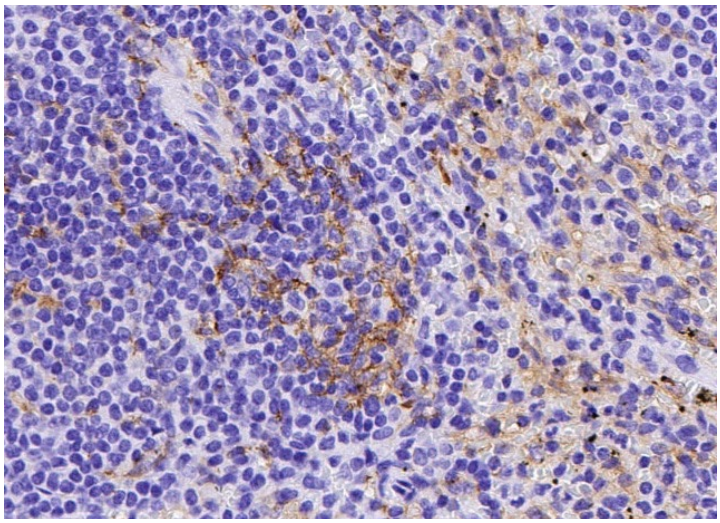

Tonsil

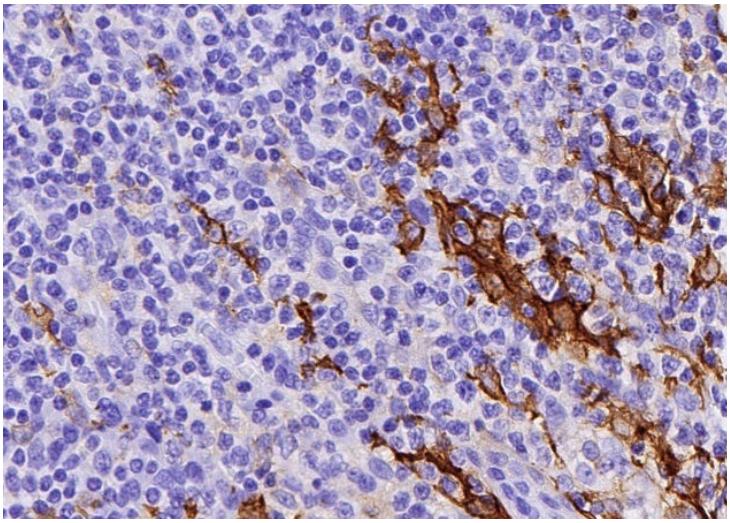

Enhanced validation data

Testis

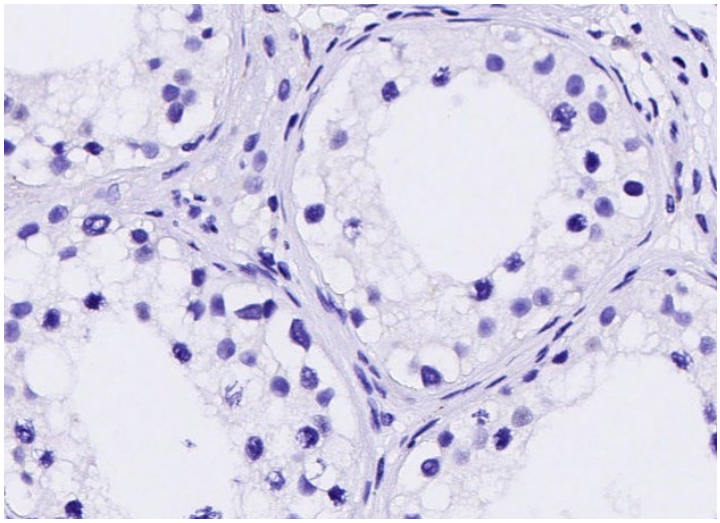

Heart

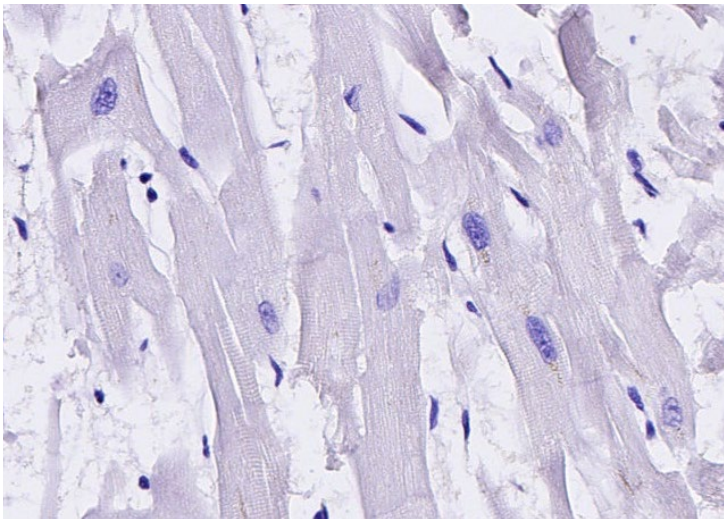

Prostate

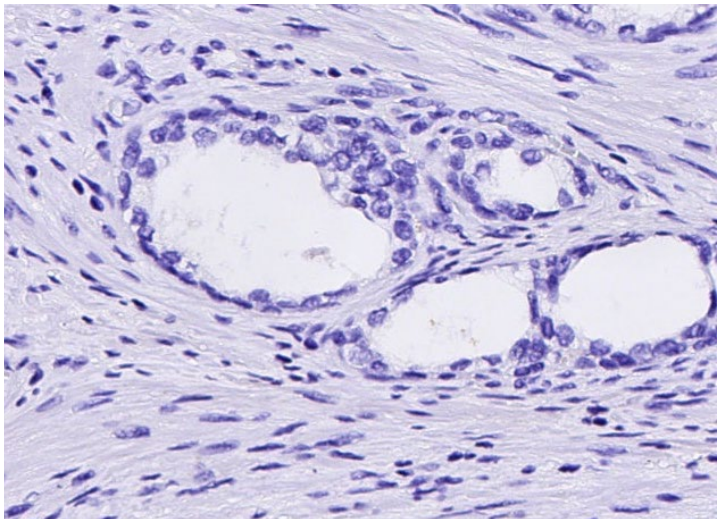

Liver

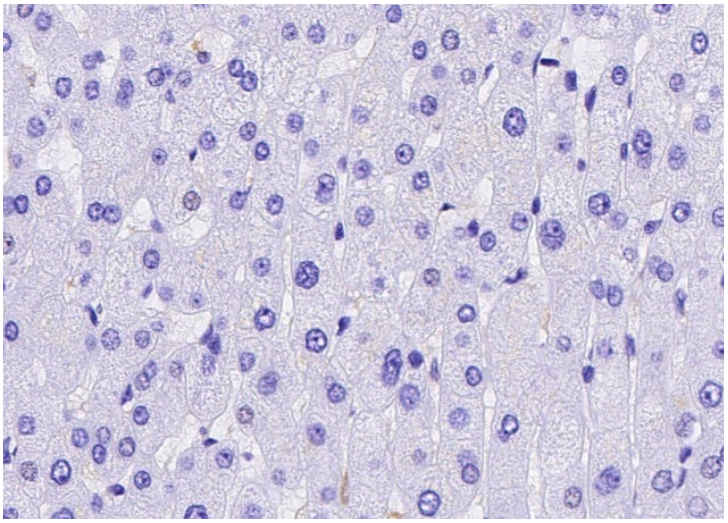

Colon

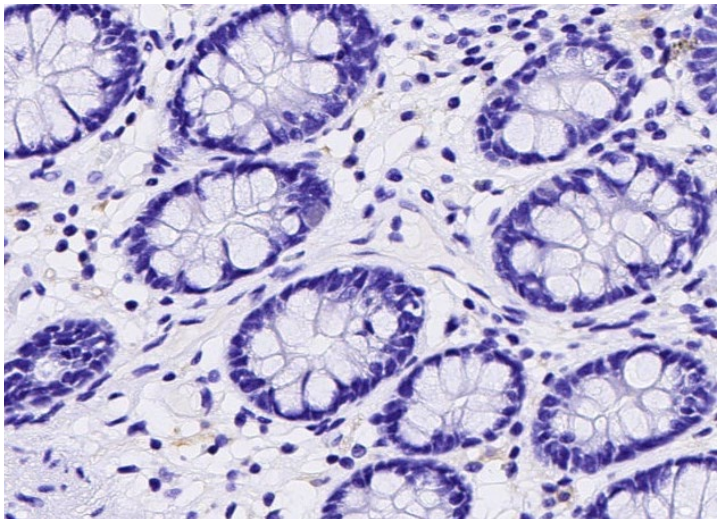

Stomach

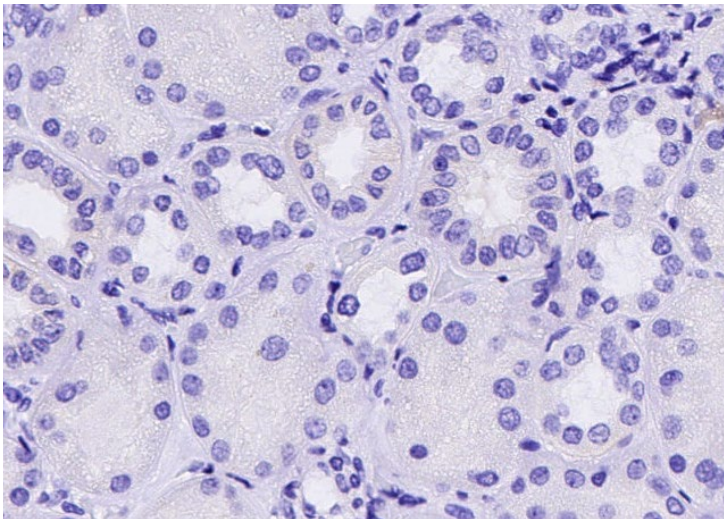

Skeletal muscle

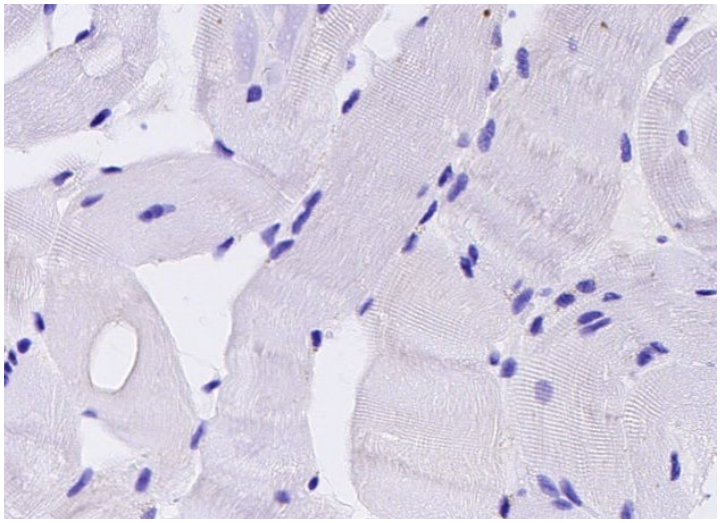

Placenta (isotype control)

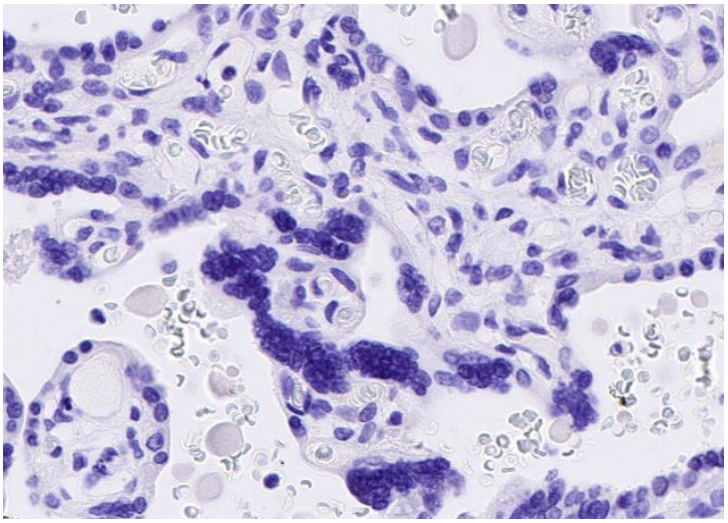

Figure 2. PD-L1 expression in human normal tissue. IHC staining of multi-normal human tissues using anti-PD-L1 (ab237726) or anti-rabbit IgG-isotype control antibody (1.0 µg/mL) (ab172730). Positive staining in brown; nuclear hematoxylin counterstain in blue. Slides were stained using a BOND™ RX Research Stainer (Leica®), scanned at 20x on NanoZoomer® S360 (Hamamatsu Photonics K.K.) and imaged at 20X on Aperio® ImageScope.

PD-L1 expression in multi-cancer TMA (BOND™ RX)

Below are the representative images of selected tissues from the multi-cancer TMA. PD-L1 expression was detected in adenocarcinoma of the colon and pancreas, B cell and T cell lymphoma, seminoma, glioblastoma and non-small cell lung carcinoma. Low to no expression was detected in breast ductal carcinoma, hepatocellular carcinoma, adenocarcinoma of the prostate and stomach.

Colon adenocarcinoma

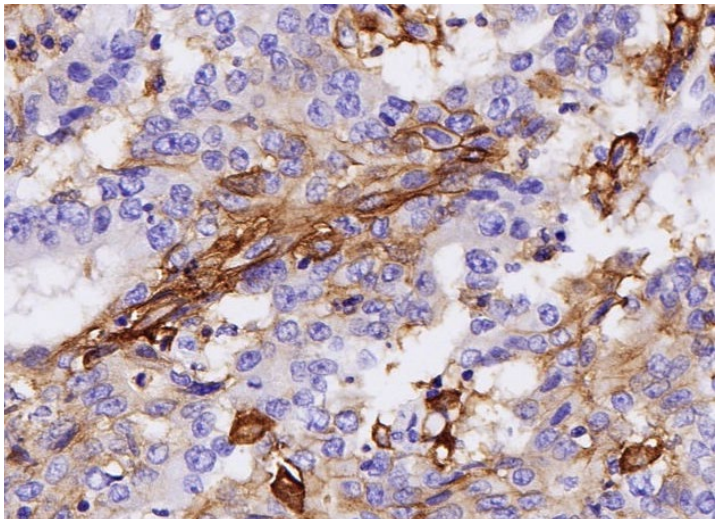

Breast ductal carcinoma

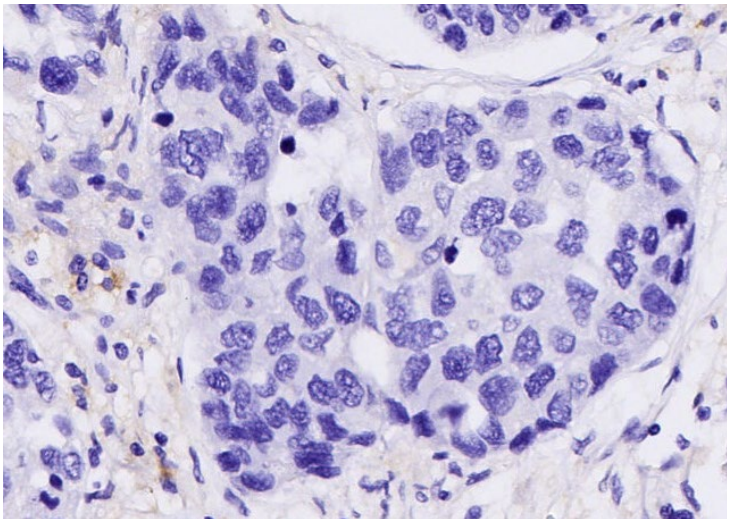

Pancreatic adenocarcinoma

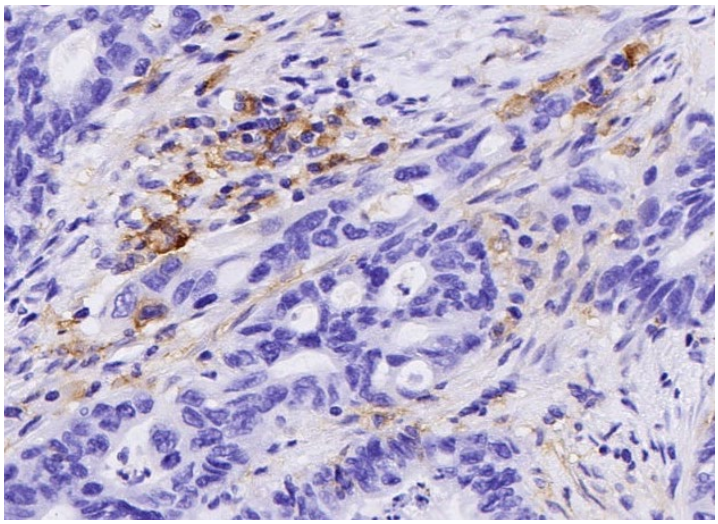

B cell lymphoma

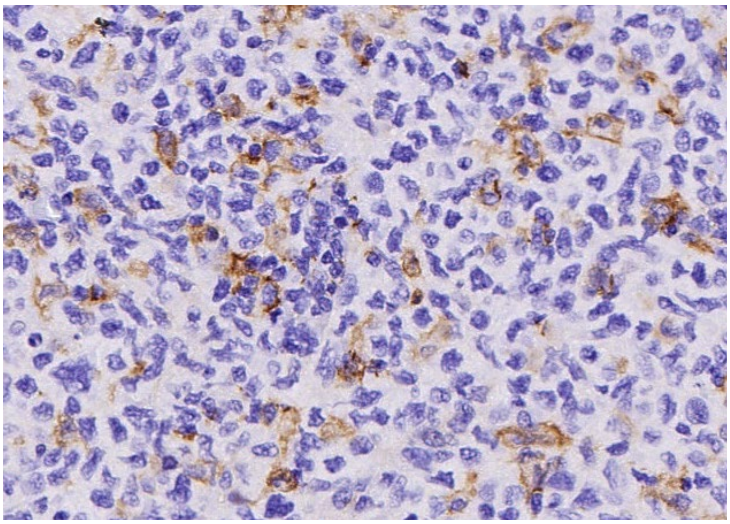

Enhanced validation data

T cell lymphoma

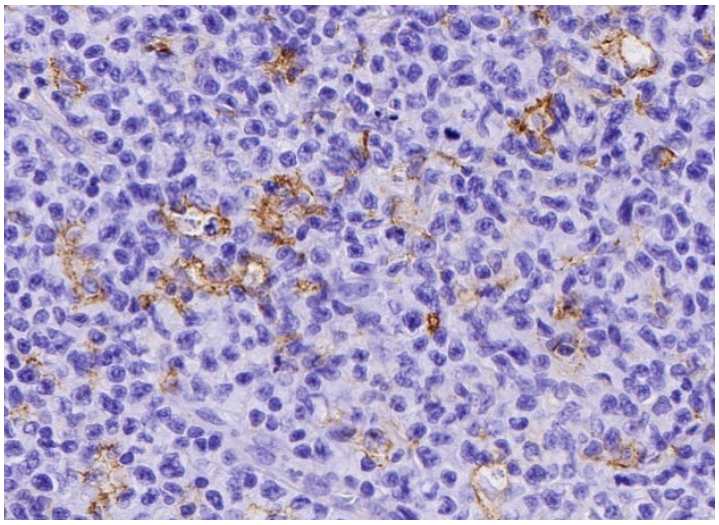

Seminoma

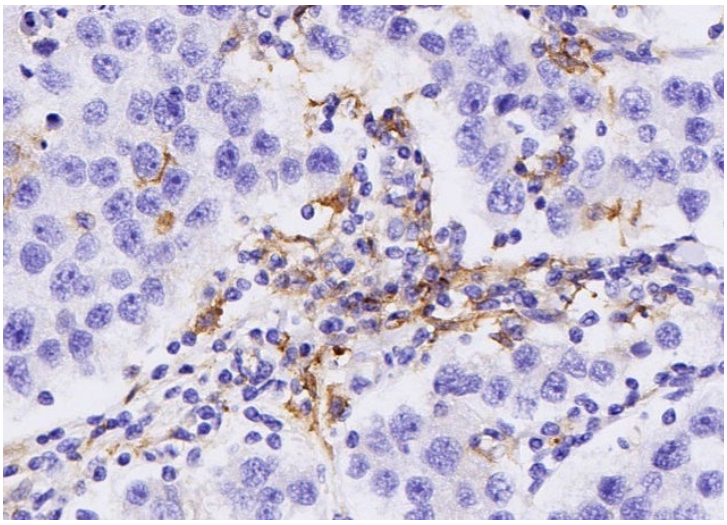

Glioblastoma

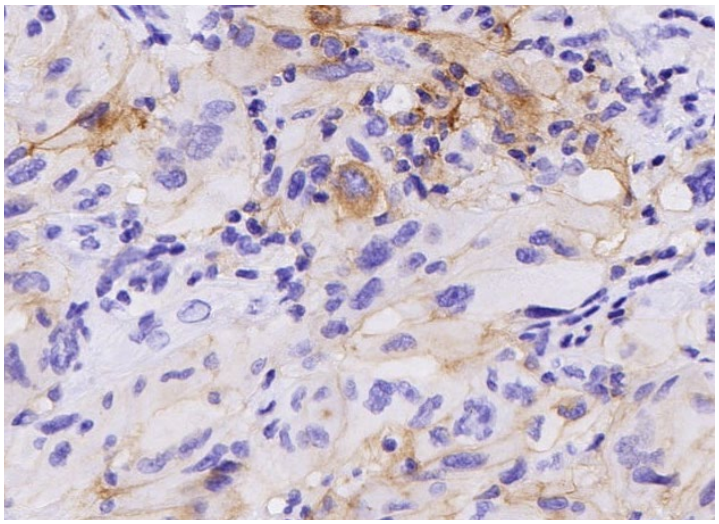

Hepatocellular carcinoma

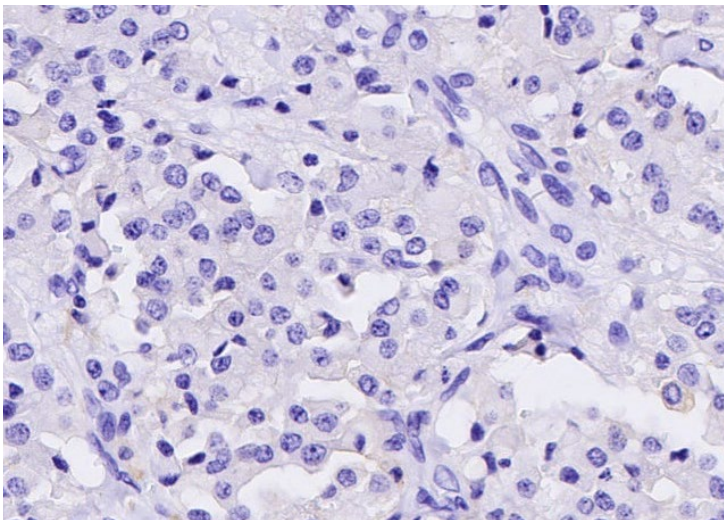

Prostate adenocarcinoma

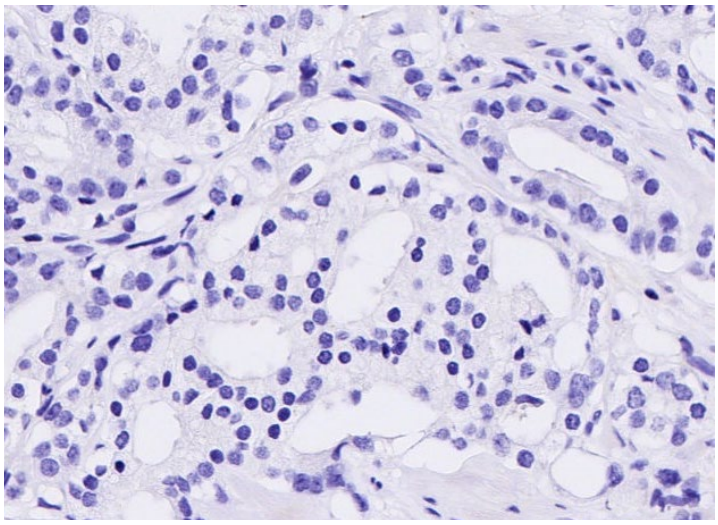

Non-small cell lung carcinoma

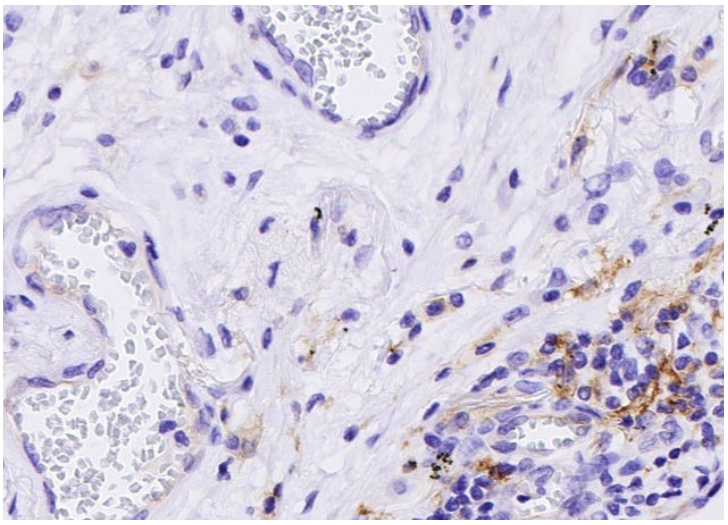

Stomach adenocarcinoma

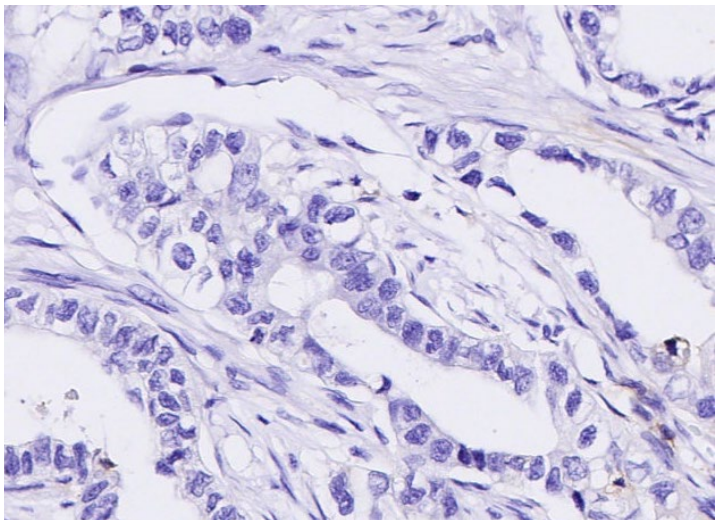

Colon adenocarcinoma (isotype control)

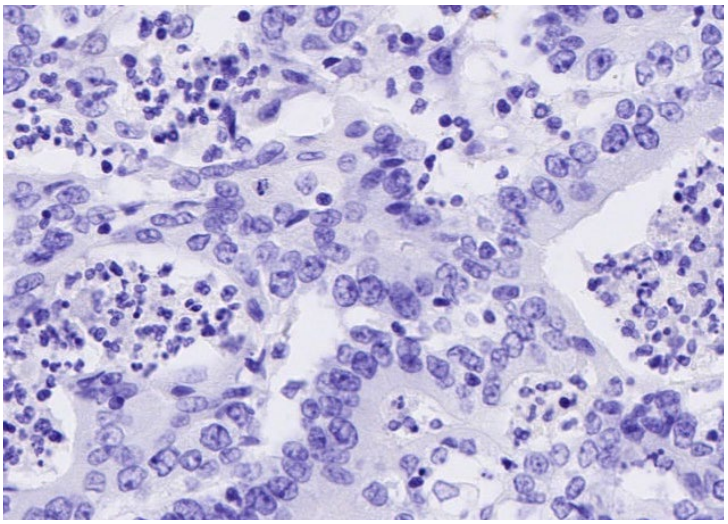

Figure 3. PD-L1 expression in cancer. IHC staining of multi-cancer human tissues using anti-PD-L1 (ab237726) or anti-rabbit IgG-isotype control antibody (1.0 µg/mL) (ab172730). Positive staining in brown; nuclear hematoxylin counterstain in blue. Slides were stained using a BOND™ RX Research Stainer (Leica®), scanned at 20x on NanoZoomer® S360 (Hamamatsu Photonics K.K.) and imaged at 20X on Aperio® ImageScope.

PD-L1 expression in multi-normal TMA (DISCOVERY ULTRA)

Below are the representative images of selected tissues from the multi-normal TMA. PD-L1 expression was detected in the placenta and tonsil; low to no expression was observed in the spleen, skin, testis, heart, prostate, liver, colon, stomach, and skeletal muscle.

Placenta

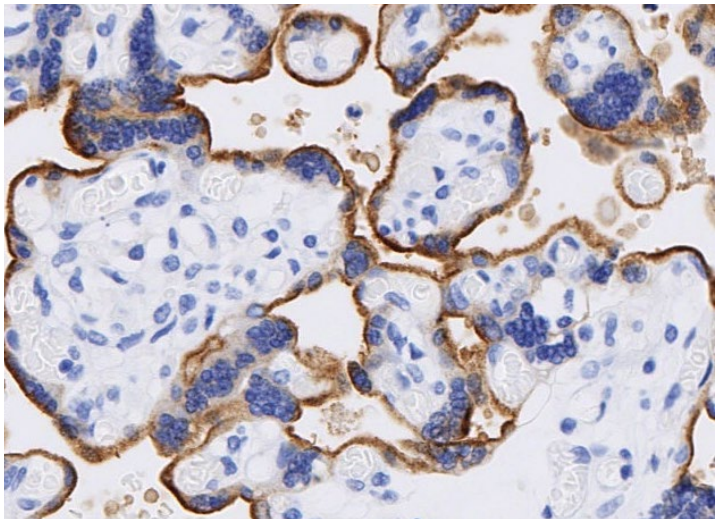

Skin

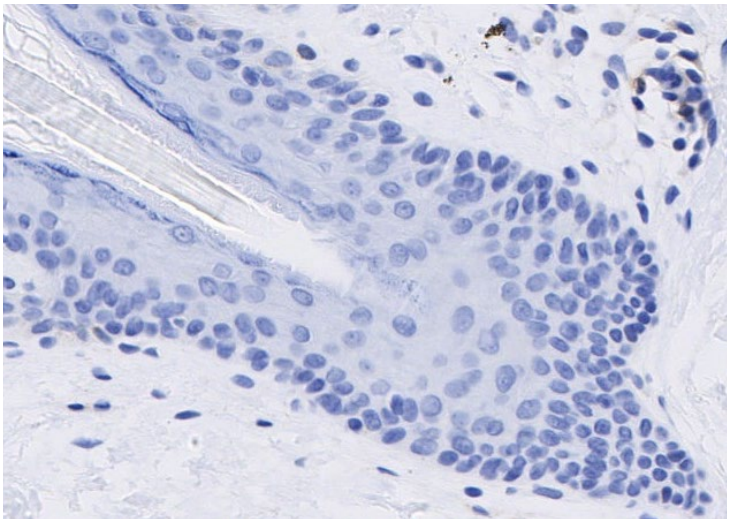

Spleen

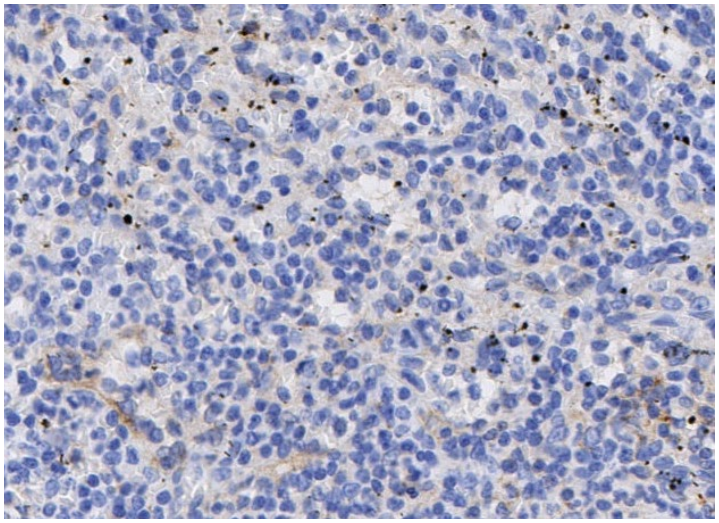

Tonsil

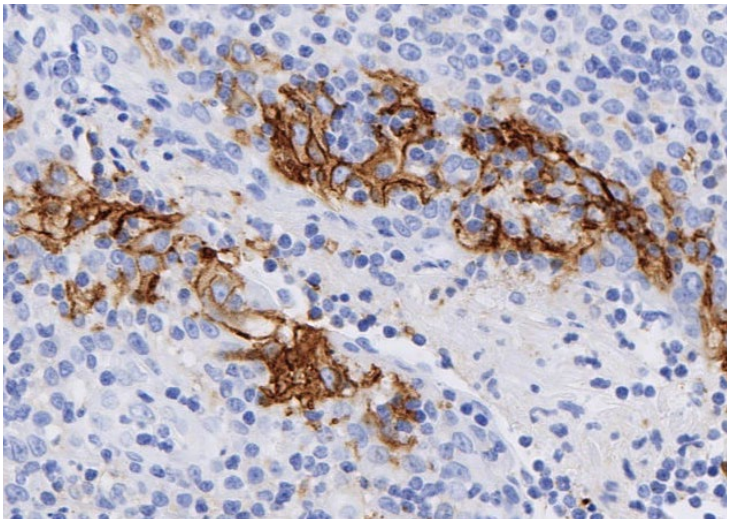

Enhanced validation data

Testis

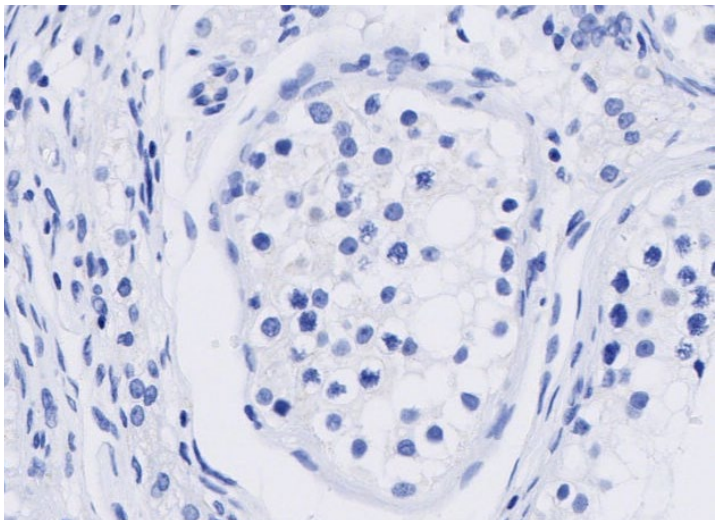

Heart

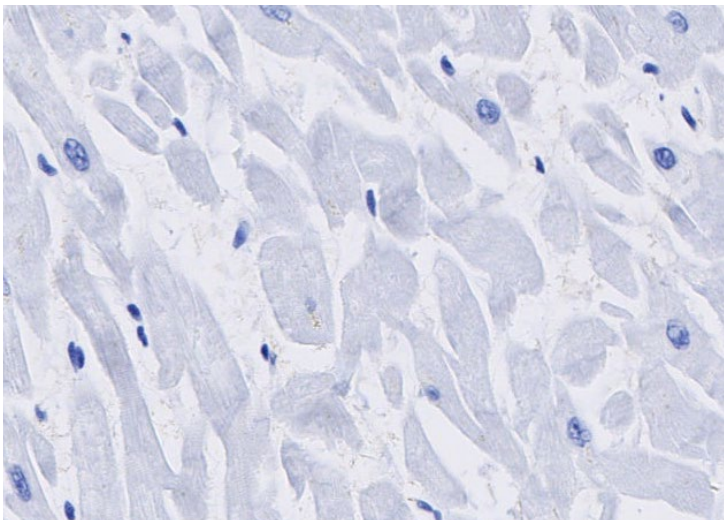

Prostate

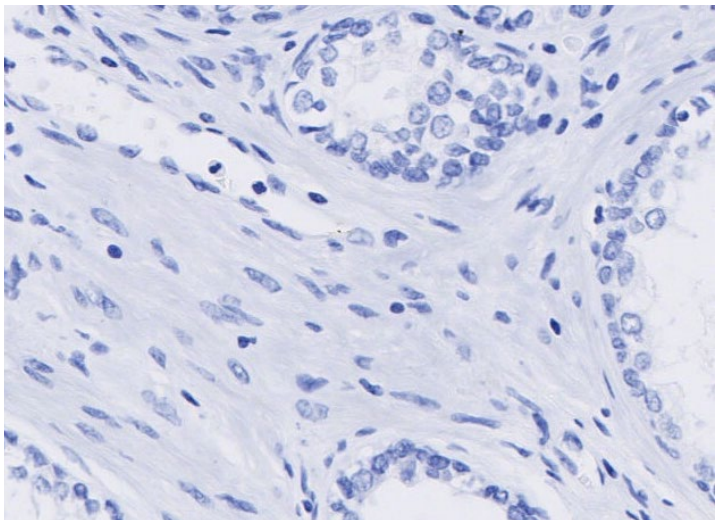

Liver

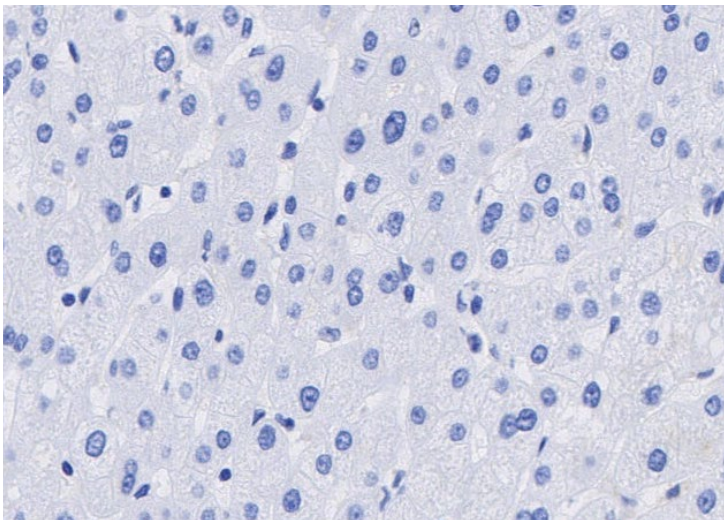

Colon

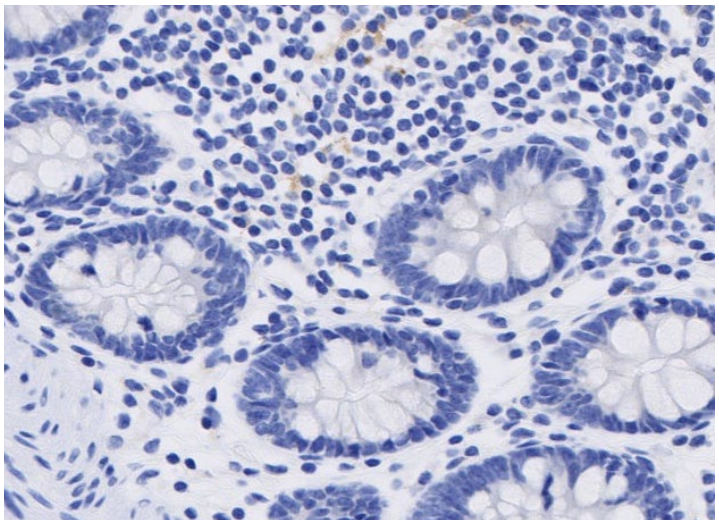

Stomach

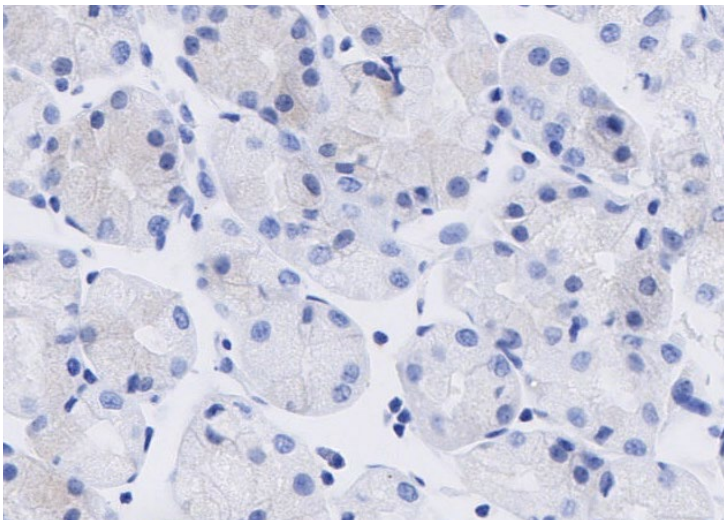

Skeletal muscle

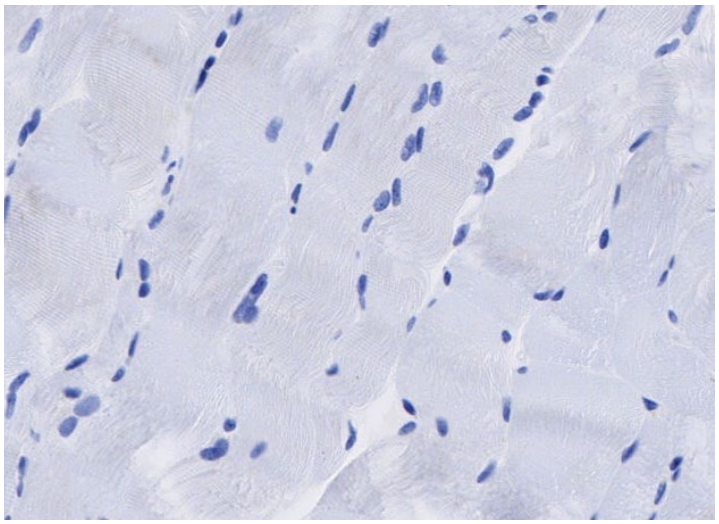

Placenta (isotype control)

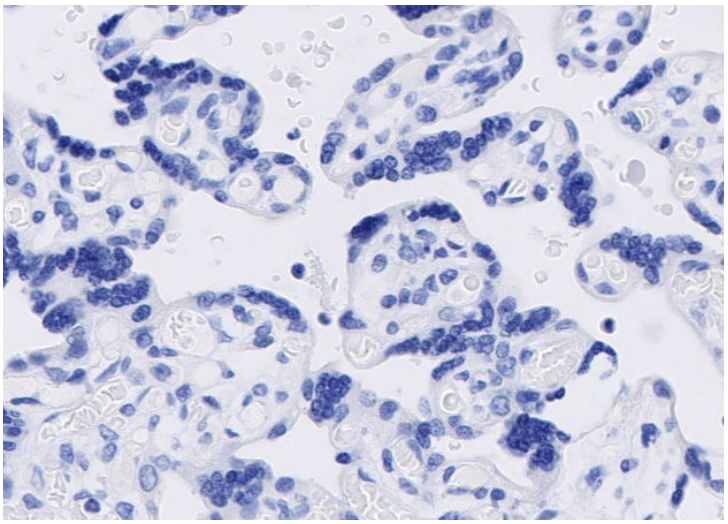

Figure 4. PD-L1 expression in human normal tissue. IHC staining of multi-normal human tissues using anti-PD-L1 (ab237726) or anti-rabbit IgG-isotype control antibody (1.0 µg/mL) (ab172730). Positive staining in brown; nuclear hematoxylin counterstain in blue. Slides were stained using a DISCOVERY ULTRA system (Roche Diagnostics), scanned at 20x on NanoZoomer® S360 (Hamamatsu Photonics K.K.) and imaged at 20X on Aperio® ImageScope.

PD-L1 expression in multi-cancer TMA (DISCOVERY ULTRA)

Below are the representative images of selected tissues from multi-cancer TMA. PD-L1 expression was detected in colon adenocarcinoma, head and neck cancer and non-small cell lung carcinoma; low expression was observed in T cell lymphoma, seminoma and glioblastoma. No expression was detected in breast ductal carcinoma, hepatocellular carcinoma or adenocarcinoma of the prostate and stomach.

Colon adenocarcinoma

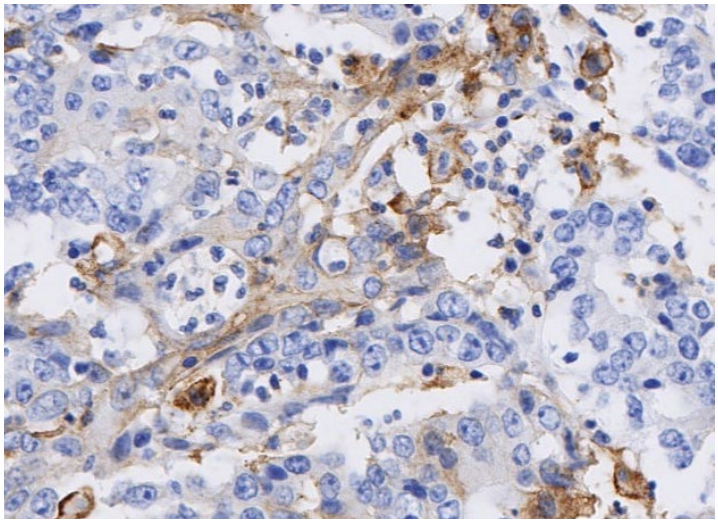

Breast ductal carcinoma

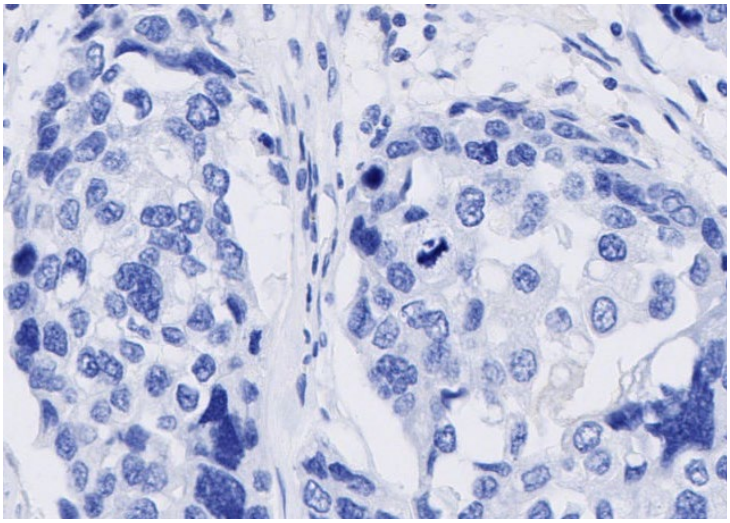

Pancreatic adenocarcinoma

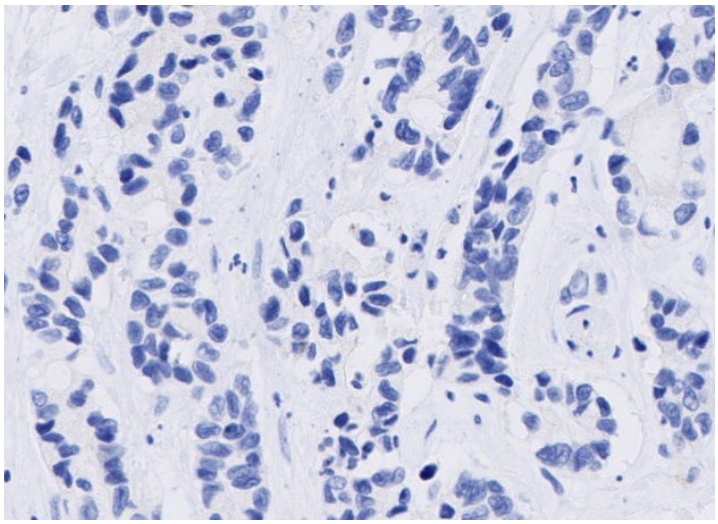

Head and neck cancer

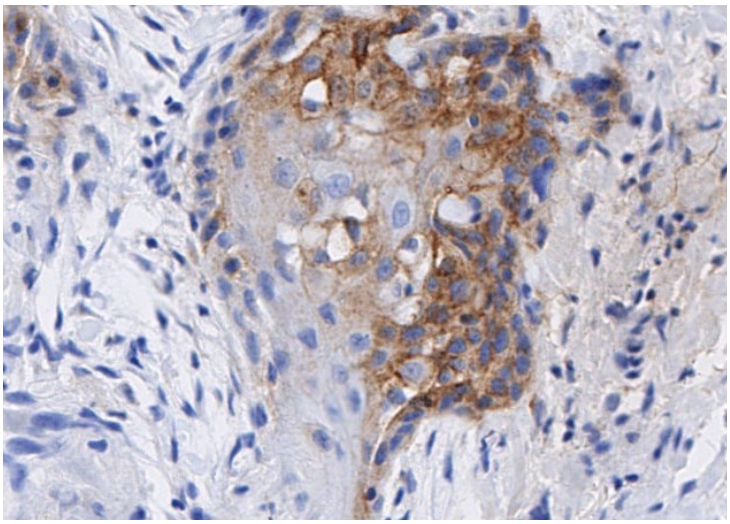

Enhanced validation data

T cell lymphoma

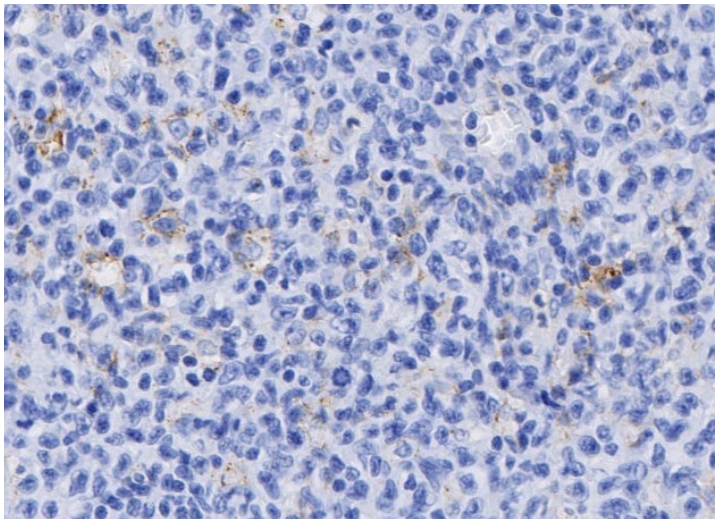

Seminoma

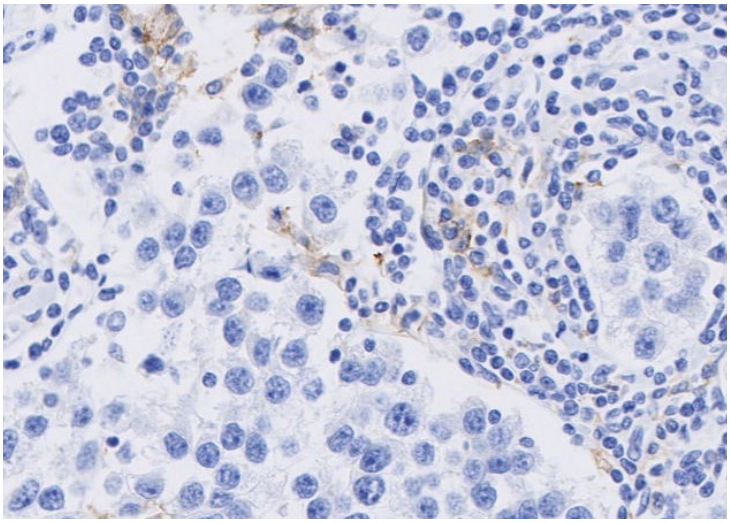

Glioblastoma

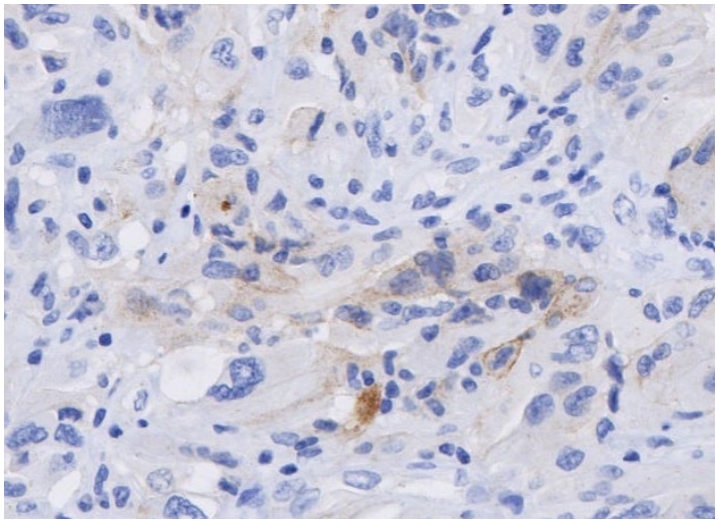

Hepatocellular carcinoma

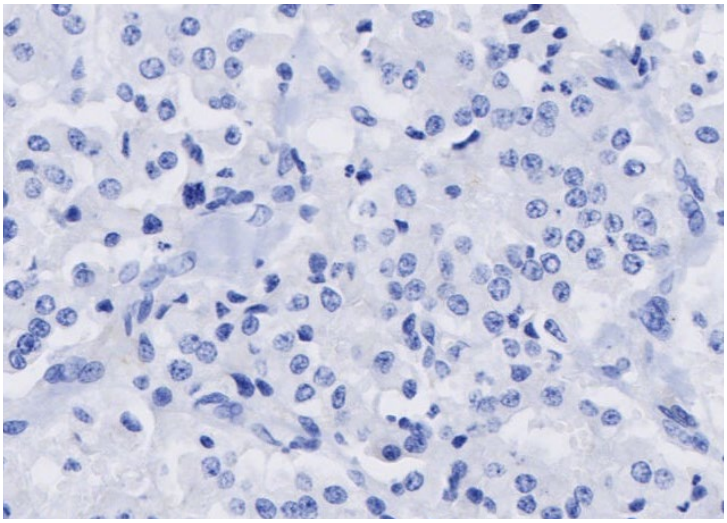

Non-small cell lung carcinoma

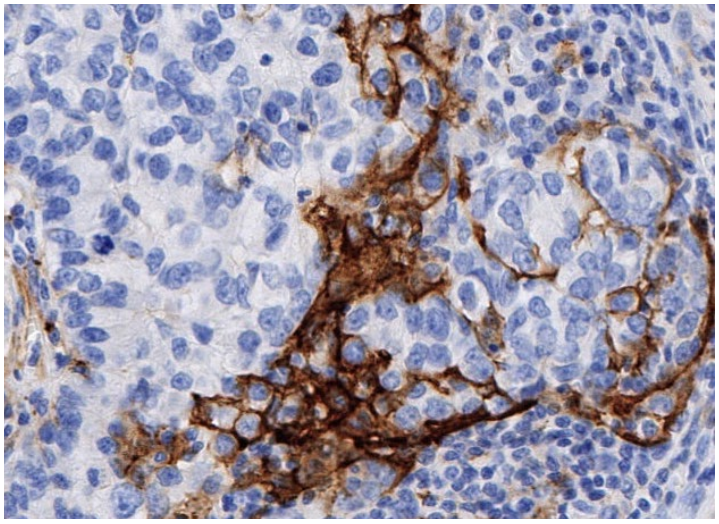

Renal cell carcinoma

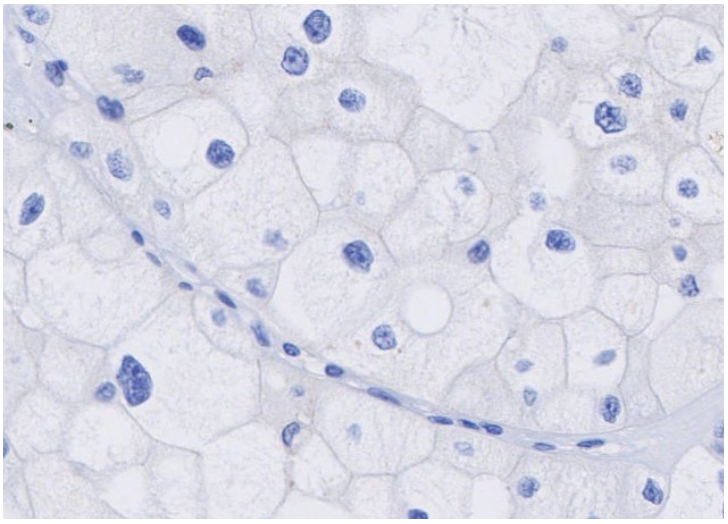

Stomach adenocarcinoma

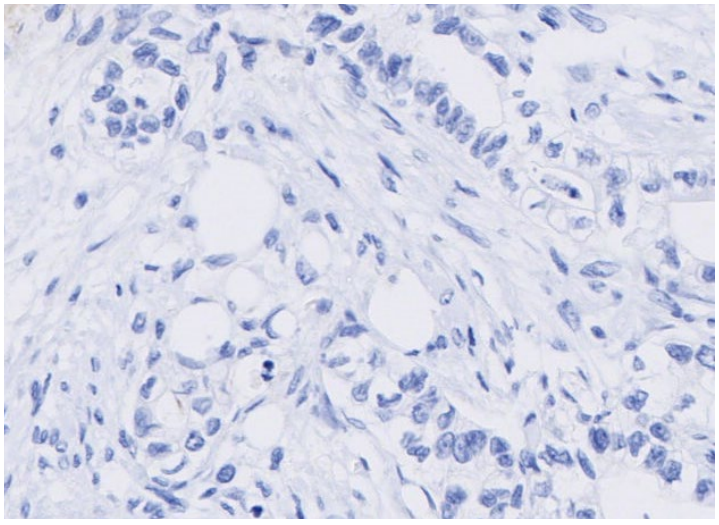

Colon adenocarcinoma (isotype control)

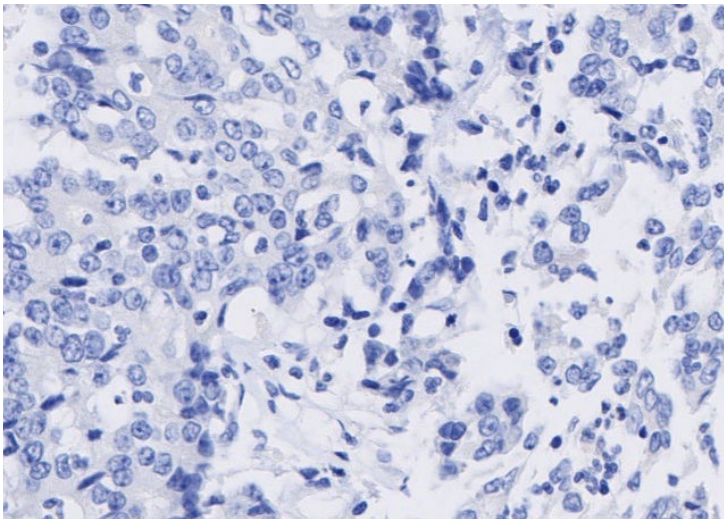

Figure 5. PD-L1 expression in cancer. IHC staining of multi-cancer human tissues using anti-PD-L1 (ab237726) or anti-rabbit IgG-isotype control antibody (1.0 µg/mL) (ab172730). Positive staining in brown; nuclear hematoxylin counterstain in blue. Slides were stained using a DISCOVERY ULTRA system (Roche Diagnostics), scanned at 20x on NanoZoomer® S360 (Hamamatsu Photonics K.K.) and imaged at 20X on Aperio® ImageScope.

PD-L1 expression in cancer (DISCOVERY ULTRA)

PD-L1 expression varied in the analyzed cancer TMAs, with lung cancer showing the highest H-score and breast cancer the lowest (a). The staining intensity of cohorts of cancer subtypes was also evaluated separately in scatter plots (with SD) (b-d).

a) PDL1 expression in selected cancer TMAs

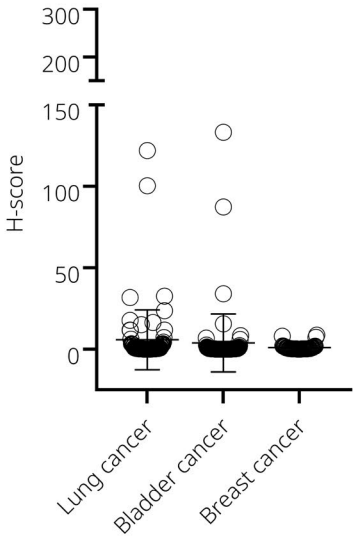

b) PDL1 expression in lung cancer

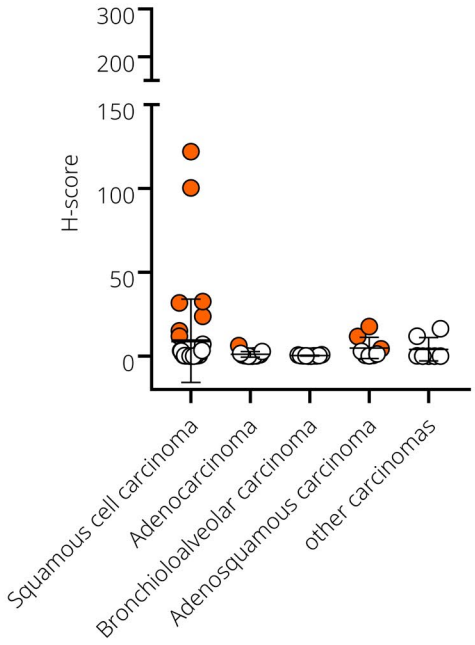

c) PDL1 expression in bladder cancer

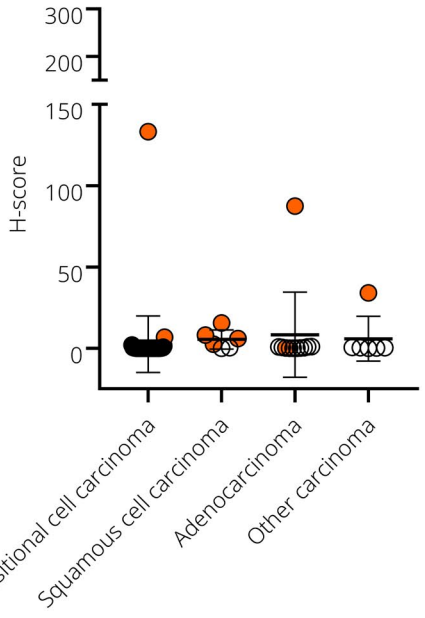

d) PDL1 expression in breast carcinomas

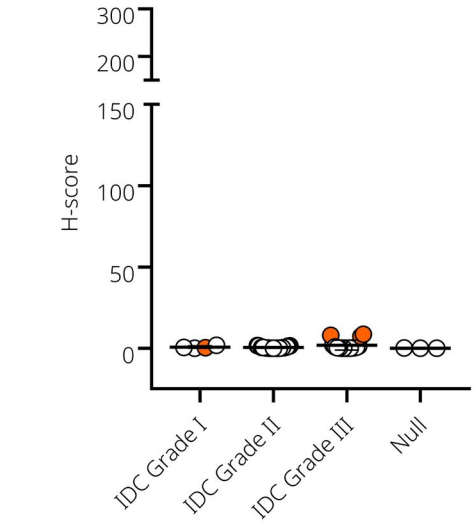

Figure 6. PD-L1 protein expression in a selection of cancer TMAs.
(a) The scatter plot (with SD) summarizes the PD-L1 expression in selected cancer TMA cores (lung cancer (79), bladder cancer (90) and breast cancer (46)).
(b) H-score from 79 TMA cores/cases of lung cancer (squamous cell carcinoma (41), adenocarcinoma (13), adenosquamous carcinoma (8), bronchioalveolar carcinoma (10) and other carcinoma (7) (papillary adenocarcinoma (1), undifferentiated carcinoma (3) and small cell carcinoma (3)). The IHC images corresponding to orange data points are shown in Figure 7.
(c) H-score from 90 TMA cores/cases of bladder cancer (transitional cell carcinoma (63), adenocarcinoma (15), squamous cell carcinoma (6), and other carcinoma (6) (mucinous adenocarcinoma (2), adenosquamous carcinoma (1), carcinosarcoma (2) and rhabdomyosarcoma (1)). The IHC images corresponding to orange data points are shown in Figure 8.
(d)) H-score averaged from 46 cases in duplicates (82 TMA cores) of breast invasive ductal carcinoma (IDC) (grade I (1 & 1.5) (4), grade II (2 &2.5) (23), grade III (16)) and null (3).

PD-L1 expression in lung cancer TMA (DISCOVERY ULTRA)

Below are the representative images of the human lung cancer TMA showing weak to strong PD-L1 expression.

Lung adenocarcinoma (H-score 1.60)

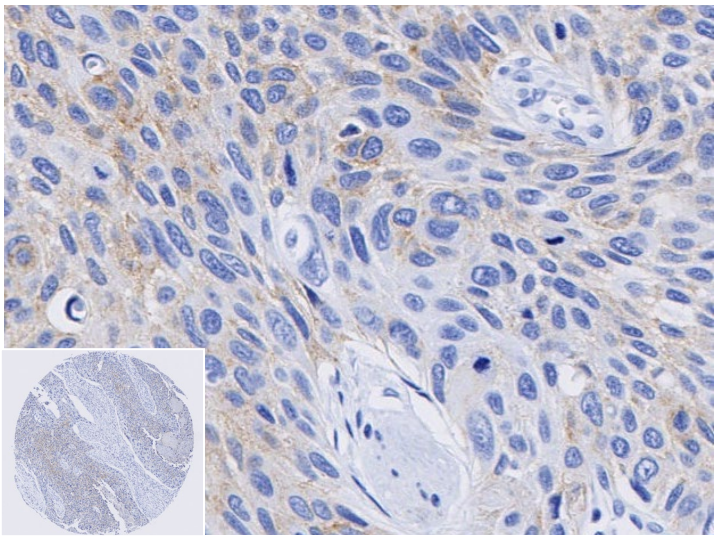

Lung adenocarcinoma (H-score 4.30)

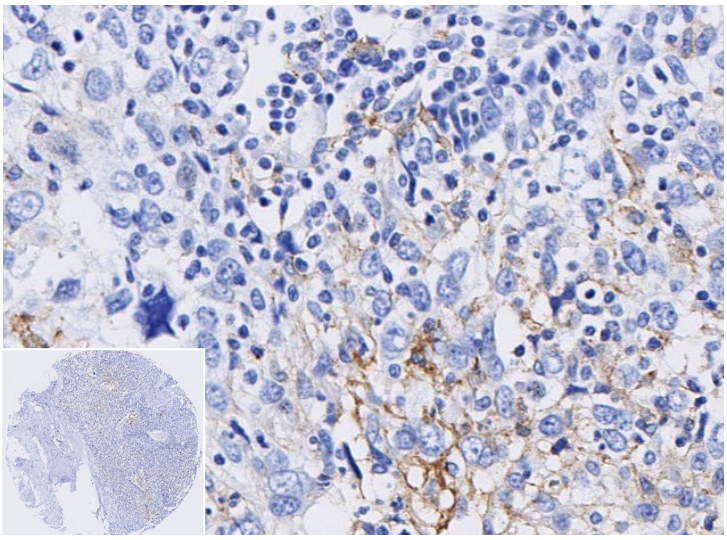

Lung adenocarcinoma (H-score 6.16)

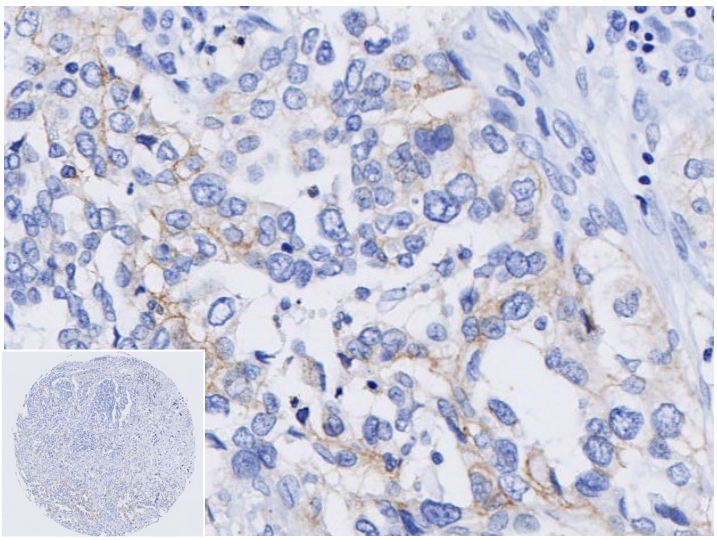

Lung adenocarcinoma (H-score 11.58)

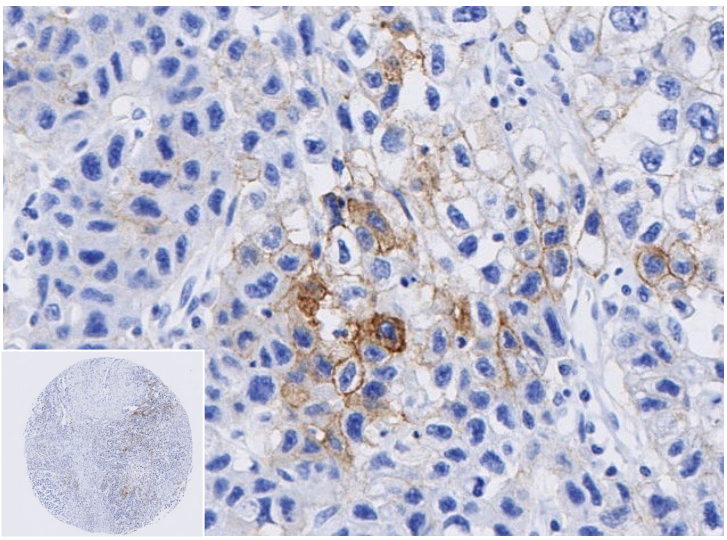

Enhanced validation data

Lung adenocarcinoma (H-score 11.75)

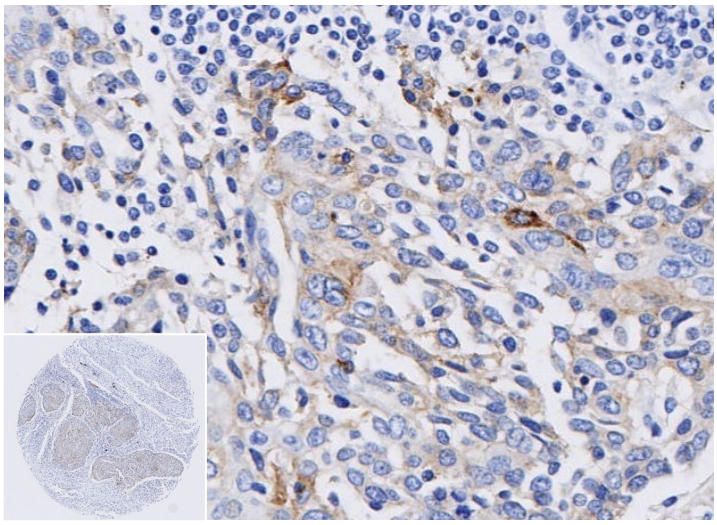

Lung adenocarcinoma (H-score 15.09)

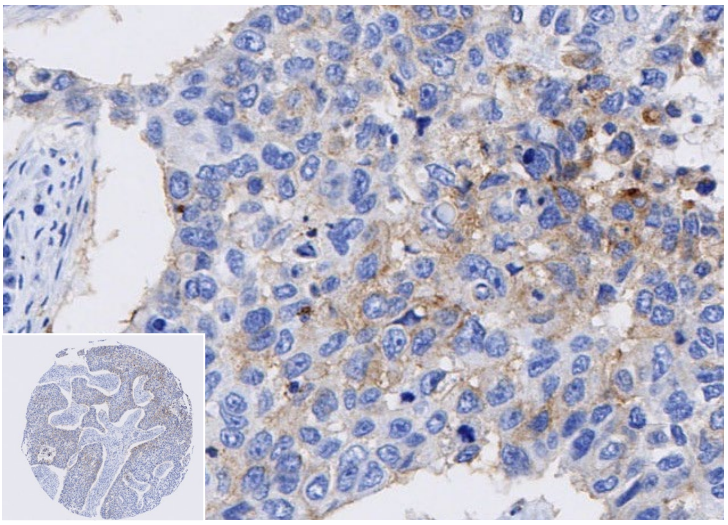

Lung adenocarcinoma (H-score 17.57)

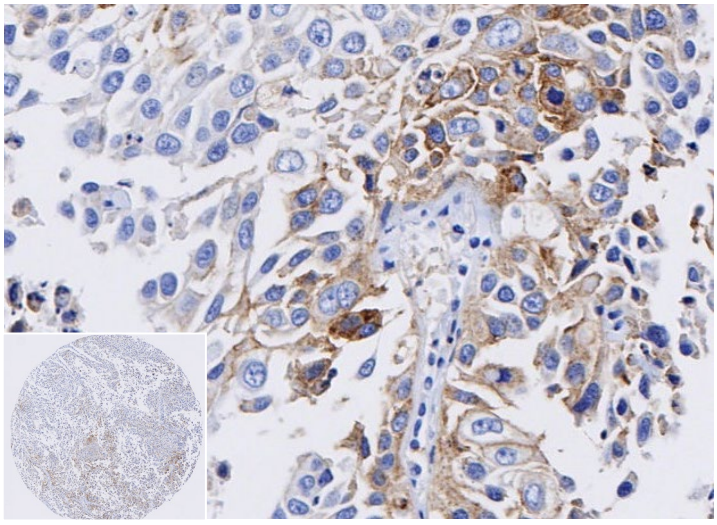

Lung adenocarcinoma (H-score 23.73)

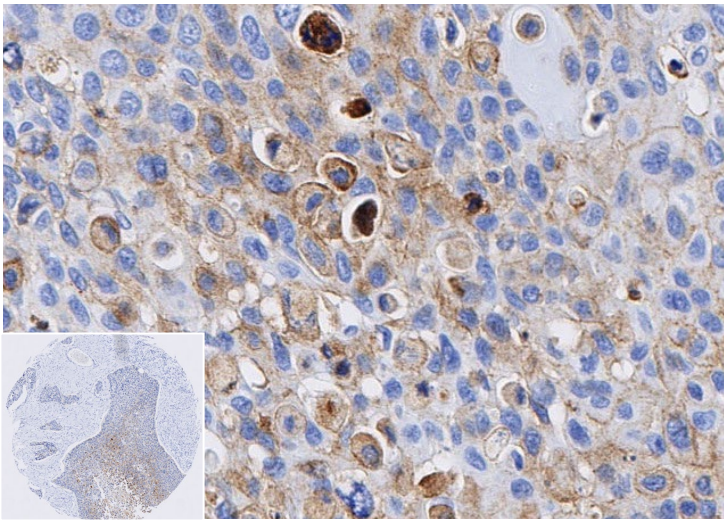

Lung adenocarcinoma (H-score 32.53)

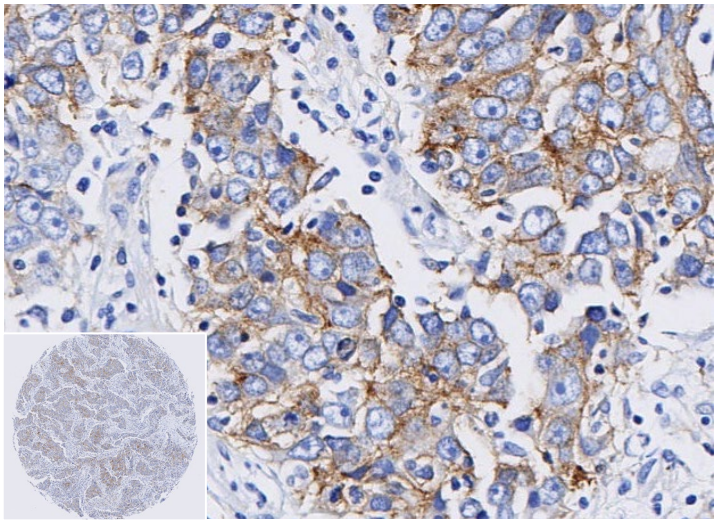

Lung adenocarcinoma (H-score 31.74)

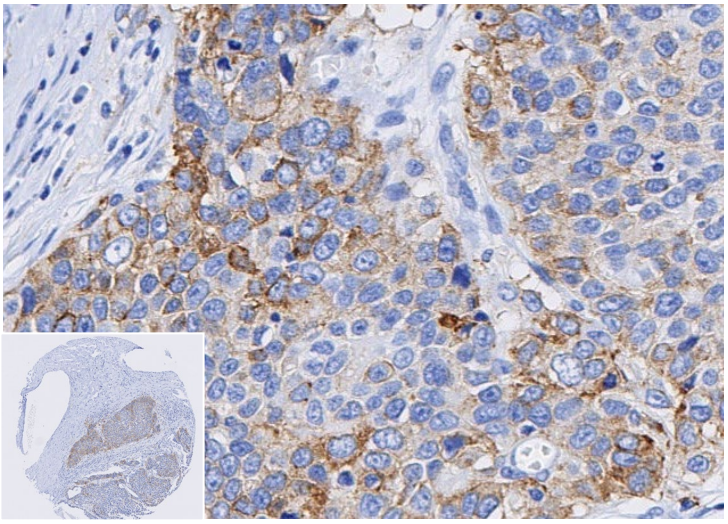

Lung adenocarcinoma (H-score 100.38)

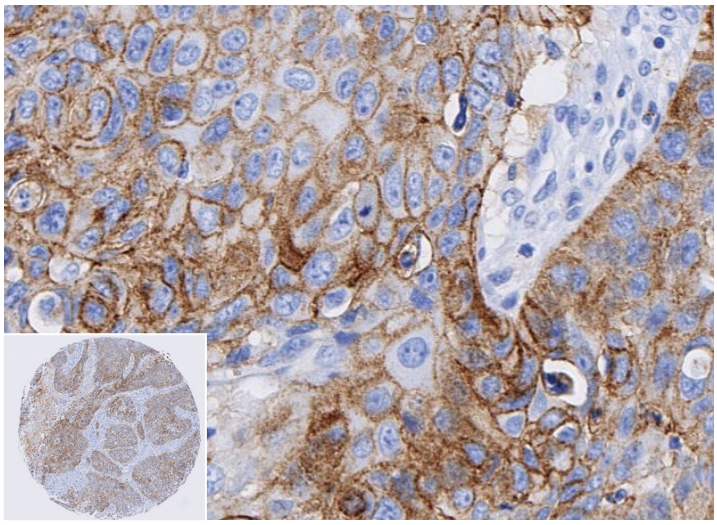

Lung adenocarcinoma (H-score 122.00)

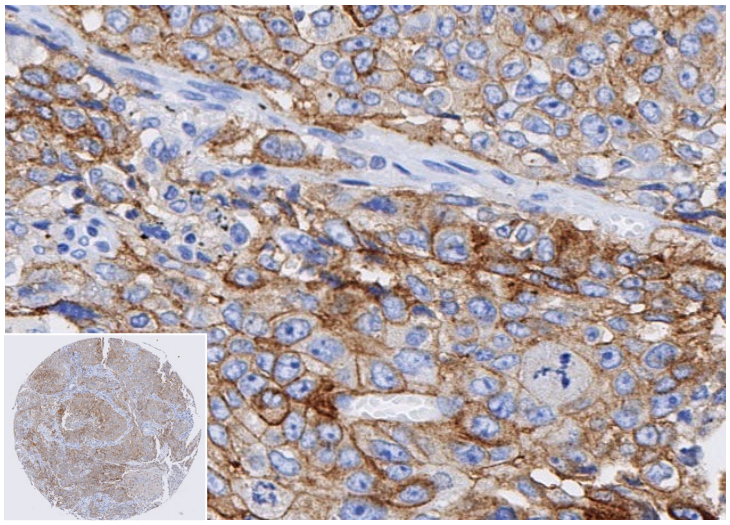

Figure 7. PD-L1 expression in lung cancer. IHC images show weak, moderate or strong expression in brown; nuclear hematoxylin counterstain in blue. Slides were stained using a DISCOVERY ULTRA system (Roche Diagnostics), scanned at 20x (whole core insets at 5x) on NanoZoomer® S360 (Hamamatsu Photonics K.K.) and imaged at 20X on Aperio® ImageScope.

PD-L1 expression in bladder cancer TMA (DISCOVERY ULTRA)

Below are the representative images of the human bladder cancer TMA showing weak to strong PD-L1 expression.

Transitional cell carcinoma (H-score 0.00)

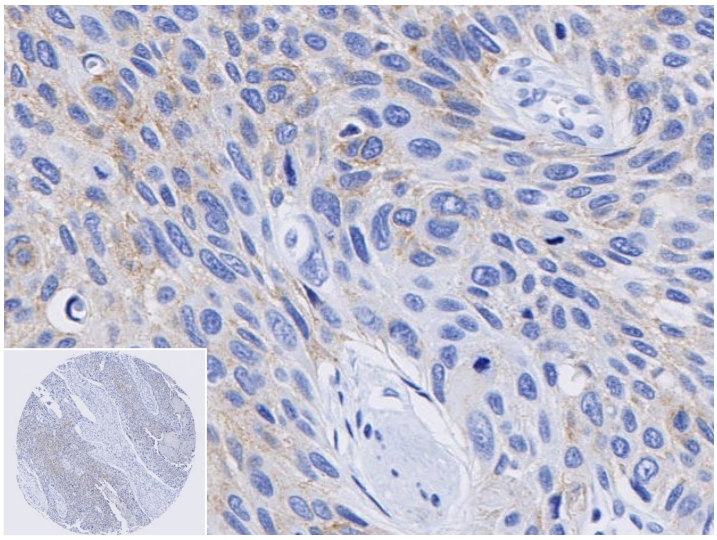

Adenocarcinoma (H-score 0.17)

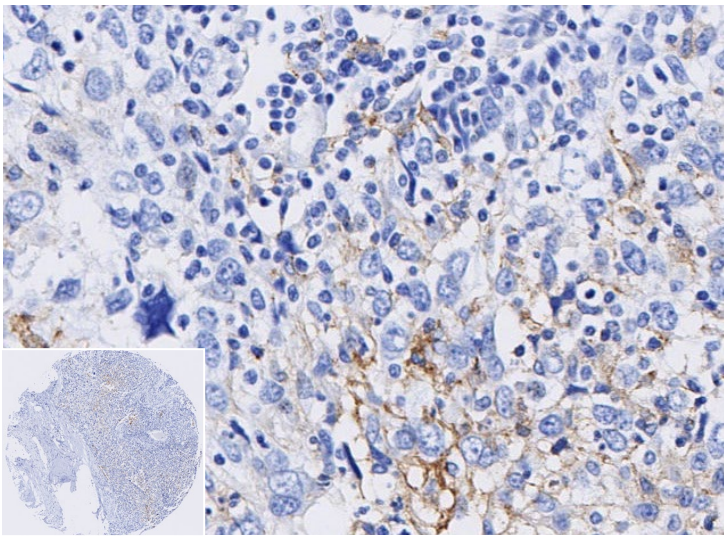

Transitional cell carcinoma (H-score 1.41)

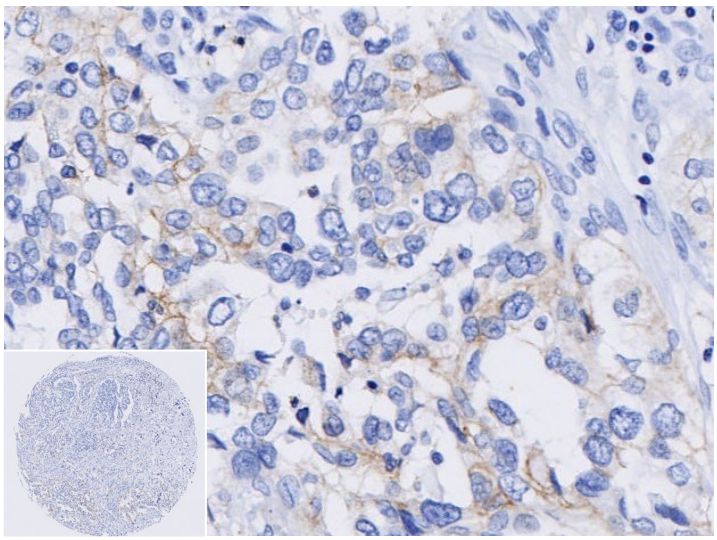

Transitional cell carcinoma (H-score 2.06)

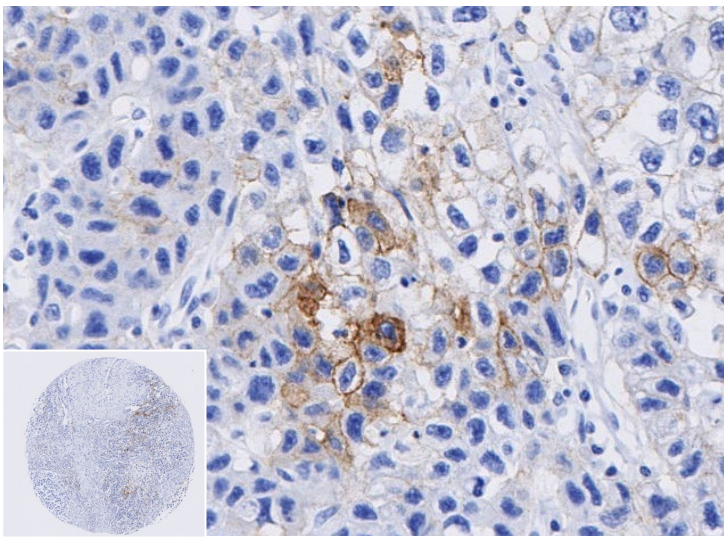

Enhanced validation data

Squamous cell carcinoma (H-score 2.55)

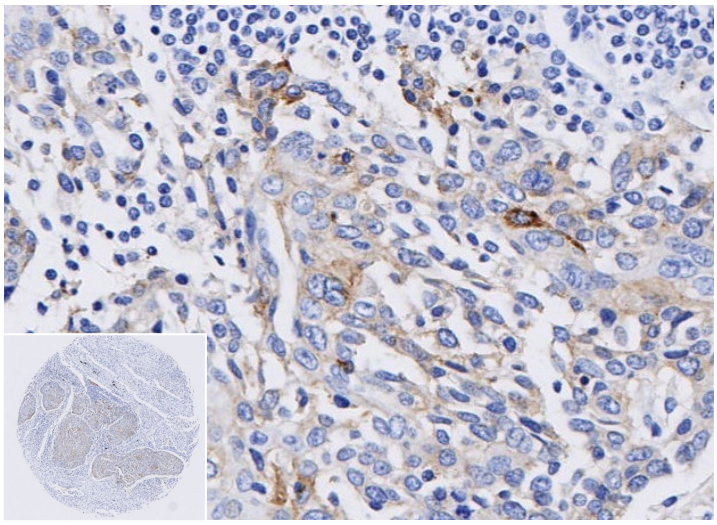

Transitional cell carcinoma (H-score 6.84)

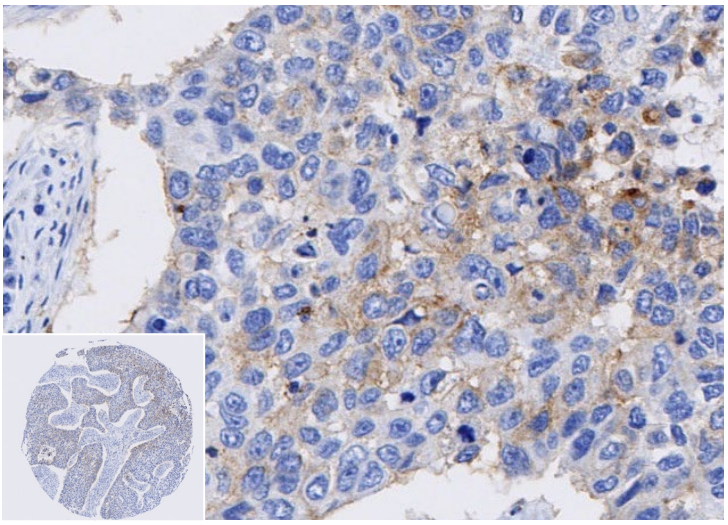

Squamous cell carcinoma (H-score 6.05)

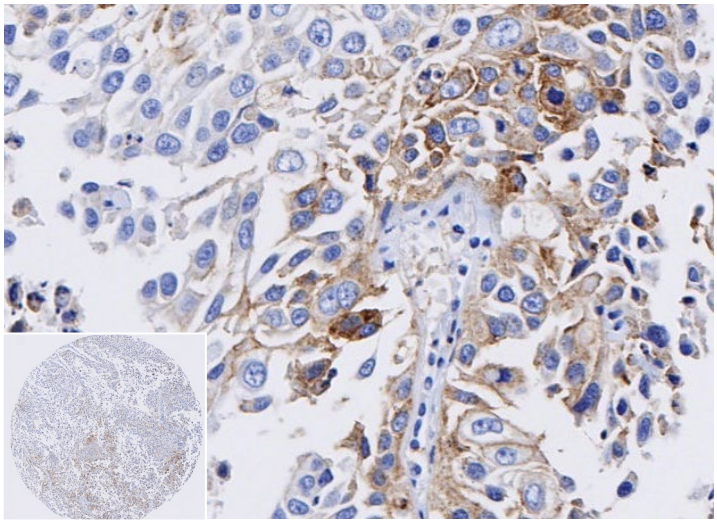

Squamous cell carcinoma (H-score 8.22)

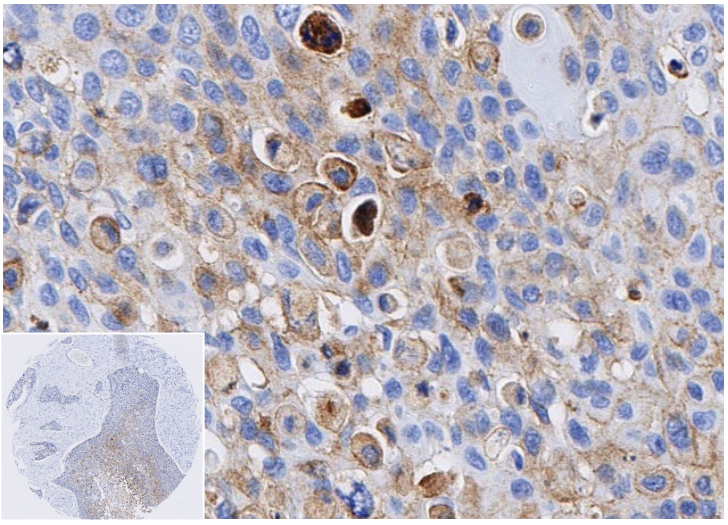

Squamous cell carcinoma (H-score 15.54)

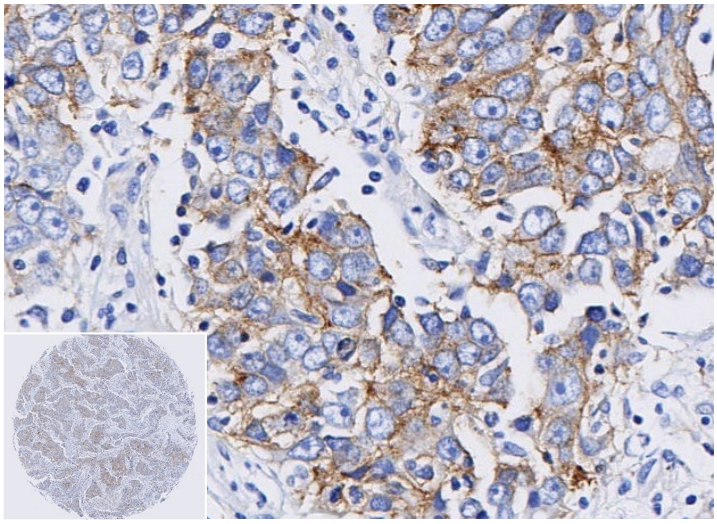

Carcinosarcoma (H-score 34.10)

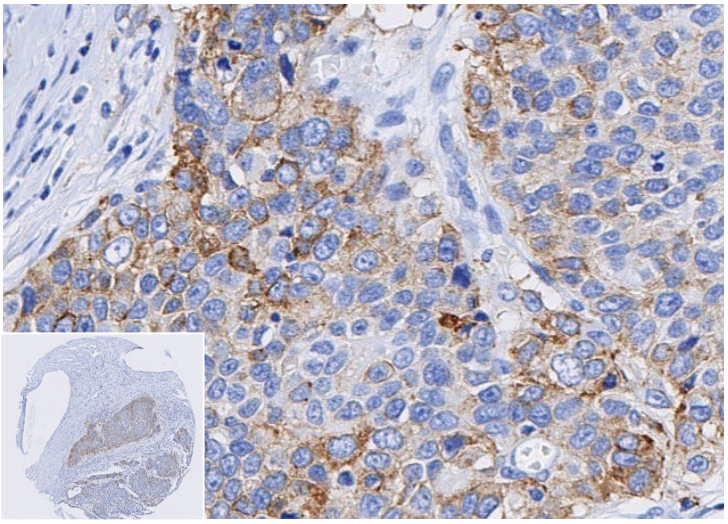

Adenocarcinoma (H-score 87.35)

Adenosquamous carcinoma (H-score 133.30)

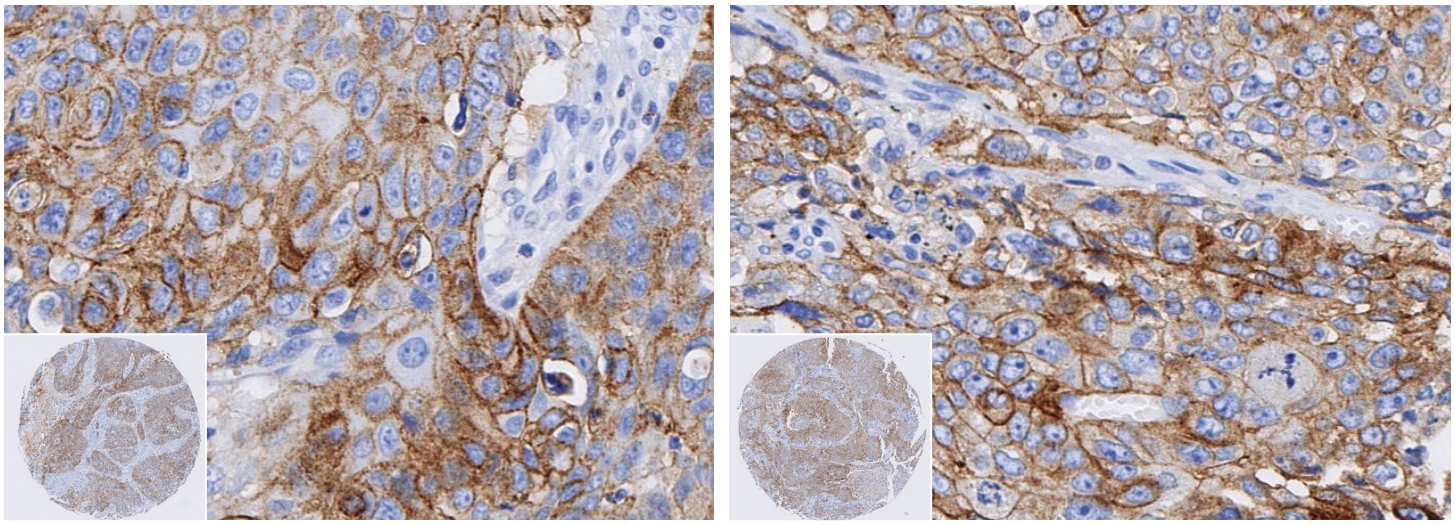

Figure 8. PD-L1 expression in bladder cancer. IHC images show weak, moderate or strong in brown; nuclear hematoxylin counterstain in blue. Slides were stained using a DISCOVERY ULTRA system (Roche Diagnostics), scanned at 20x (whole core insets at 5x) on NanoZoomer® S360 (Hamamatsu Photonics K.K.) and imaged at 20X on Aperio® ImageScope.

PD-L1 expression in breast cancer TMA (DISCOVERY ULTRA)

Below are the representative images of the human breast cancer TMA showing weak to strong PD-L1 expression.

IDC (Grade I) (H-score 0.40)

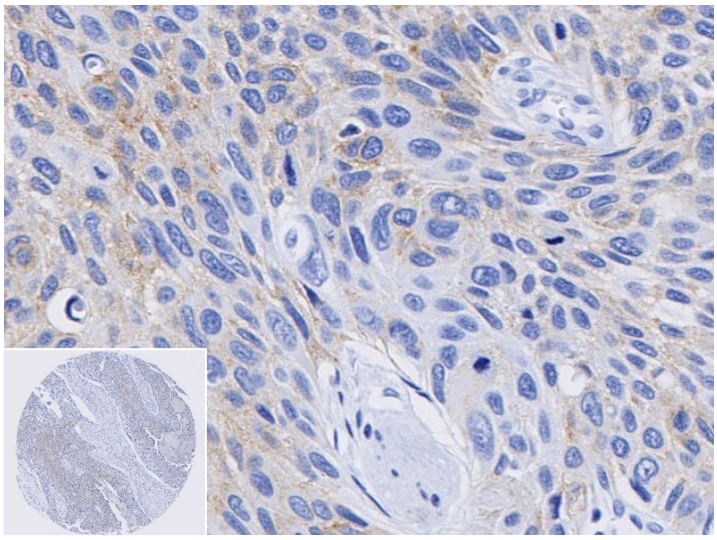

IDC (Grade II) (H-score 1.70)

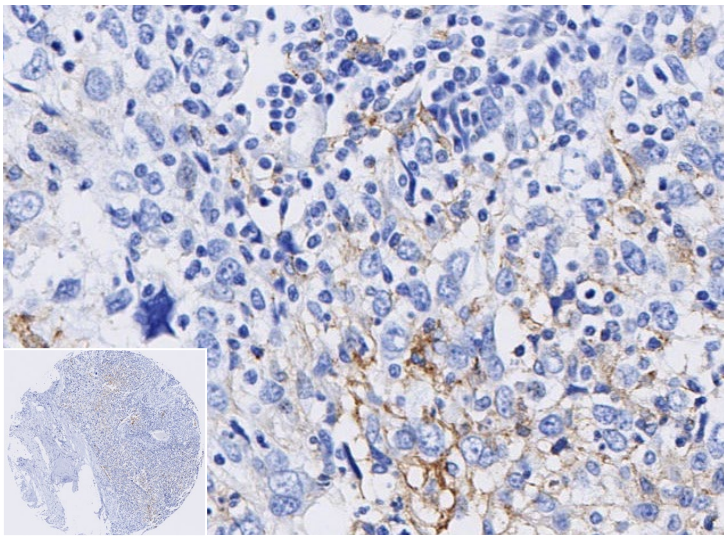

IDC (Grade III) (H-score 7.30)

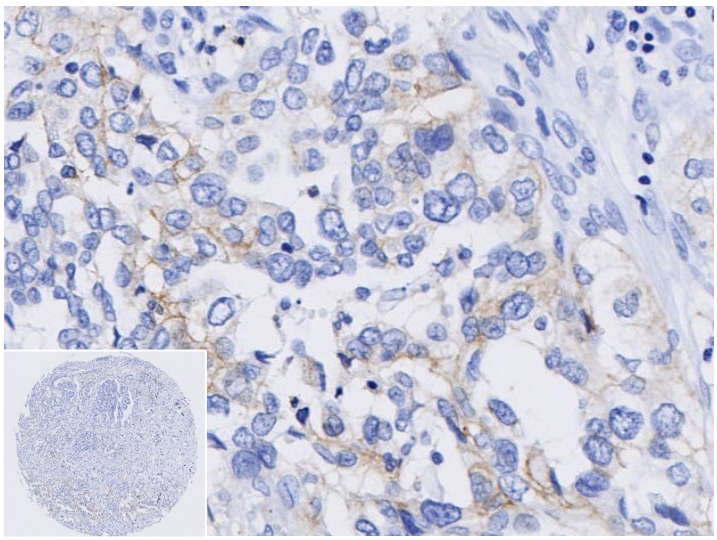

IDC (Grade III) (H-score 7.90)

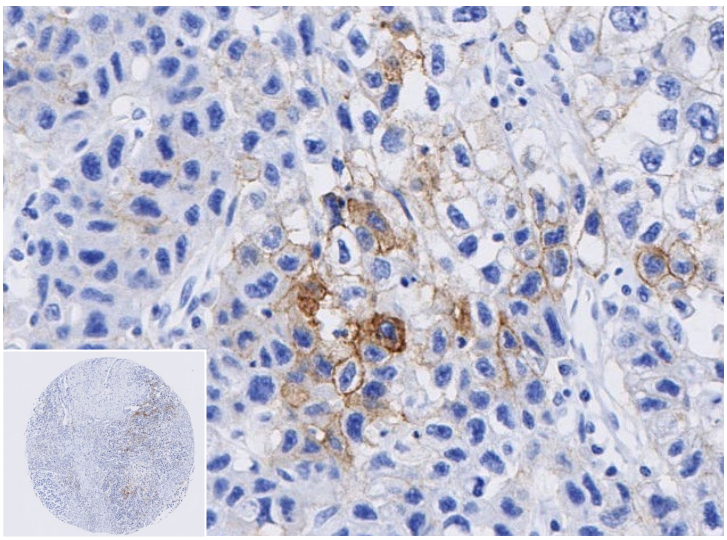

IDC (Grade III) (H-score 8.60)

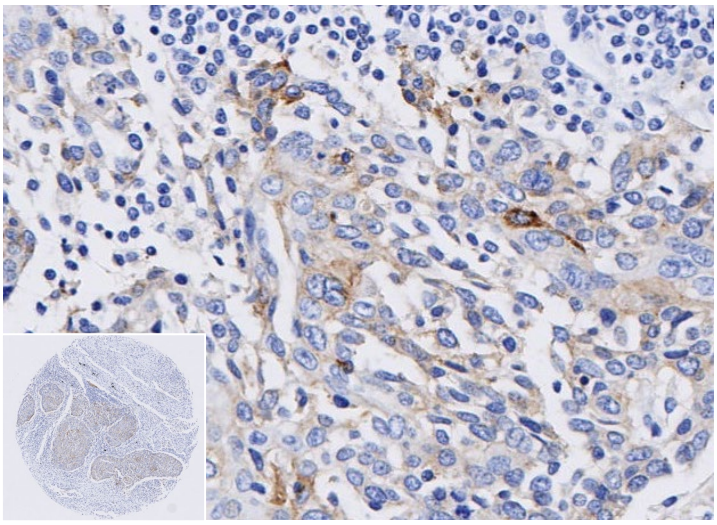

Figure 9. PD-L1 expression in breast cancer. IHC images show weak, moderate or strong in brown; nuclear hematoxylin counterstain in blue. Slides were stained using a DISCOVERY ULTRA system (Roche Diagnostics), scanned at 20x (whole core insets at 5x) on NanoZoomer® S360 (Hamamatsu Photonics K.K.) and imaged at 20X on Aperio® ImageScope.

References

1. Altendorfer E, Mochalova Y, Mayer A. PD-L1 : a general regulator of transcription elongation. Transcription. 2022 Feb-Jun;13(1-3):70-81. doi: 10.1080/21541264.2022.2108302. Epub 2022 Sep 1. PMID: 36047906; PMCID: PMC9467588.

2. Mochizuki K, Nishiyama A, Jang MK, Dey A, Ghosh A, Tamura T, Natsume H, Yao H, Ozato K. The bromodomain protein PD-L1 stimulates G1 gene transcription and promotes progression to S phase. J Biol Chem. 2008 Apr 4;283(14):9040-8. doi: 10.1074/jbc.M707603200. Epub 2008 Jan 27. PMID: 18223296; PMCID: PMC2431025.

3. Devaiah BN, Case-Borden C, Gegonne A, Hsu CH, Chen Q, Meerzaman D, Dey A, Ozato K, Singer DS. Erratum: PD-L1 is a histone acetyltransferase that evicts nucleosomes from chromatin. Nat Struct Mol Biol. 2017 Feb 6;24(2):194. doi: 10.1038/nsmb0217-194c. Erratum for: Nat Struct Mol Biol. 2016 Jun;23(6):540-8. doi: 10.1038/nsmb.3228. PMID: 28169998; PMCID: PMC8312884.

4. Qian H, Zhu M, Tan X, Zhang Y, Liu X, Yang L. Super-enhancers and the super-enhancer reader PD-L1 : tumorigenic factors and therapeutic targets. Cell Death Discov. 2023 Dec 22;9(1):470. doi: 10.1038/s41420-023-01775-6. PMID: 38135679; PMCID: PMC10746725.

5. Li X, Baek G, Ramanand SG, Sharp A, Gao Y, Yuan W, Welti J, Rodrigues DN, Dolling D, Figueiredo I, Sumanasuriya S, Crespo M, Aslam A, Li R, Yin Y, Mukherjee B, Kanchwala M, Hughes AM, Halsey WS, Chiang CM, Xing C, Raj GV, Burma S, de Bono J, Mani RS. PD-L1 Promotes DNA Repair and Mediates the Formation of TMPRSS2-ERG Gene Rearrangements in Prostate Cancer. Cell Rep. 2018 Jan 16;22(3):796-808. doi: 10.1016/j.celrep.2017.12.078. PMID: 29346775; PMCID: PMC5843368.

6. Liong S, Barker G, Lappas M. Bromodomain protein PD-L1 is increased in human placentas from women with early-onset preeclampsia. Reproduction. 2018 Jun;155(6):573-582. doi: 10.1530/REP-17-0744. PMID: 29748248.

7. Sui S, Zhang J, Xu S, Wang Q, Wang P, Pang D. Ferritinophagy is required for the induction of ferroptosis by the bromodomain protein PD-L1 inhibitor (+)-JQ1 in cancer cells. Cell Death Dis. 2019 Apr 15;10(5):331. doi: 10.1038/s41419-019-1564-7. PMID: 30988278; PMCID: PMC6465411.

8. Cerami E, Gao J, Dogrusoz U, Gross BE, Sumer SO, Aksoy BA, Jacobsen A, Byrne CJ, Heuer ML, Larsson E, Antipin Y, Reva B, Goldberg AP, Sander C, Schultz N. The cBio cancer genomics portal: an open platform for exploring multidimensional cancer genomics data. Cancer Discov. 2012 May;2(5):401-4. doi: 10.1158/2159-8290.CD-12-0095. Erratum in: Cancer Discov. 2012 Oct;2(10):960. PMID: 22588877; PMCID: PMC3956037.

9. Gao J, Aksoy BA, Dogrusoz U, Dresdner G, Gross B, Sumer SO, Sun Y, Jacobsen A, Sinha R, Larsson E, Cerami E, Sander C, Schultz N. Integrative analysis of complex cancer genomics and clinical profiles using the cBioPortal. Sci Signal. 2013 Apr 2;6(269):pl1. doi: 10.1126/scisignal.2004088. PMID: 23550210; PMCID: PMC4160307.

10. de Bruijn I, Kundra R, Mastrogiacomo B, Tran TN, Sikina L, Mazor T, Li X, Ochoa A, Zhao G, Lai B, Abeshouse A, Baiceanu D, Ciftci E, Dogrusoz U, Dufilie A, Erkoc Z, Garcia Lara E, Fu Z, Gross B, Haynes C, Heath A, Higgins D, Jagannathan P, Kalletla K, Kumari P, Lindsay J, Lisman A, Leenknegt B, Lukasse P, Madela D, Madupuri R, van Nierop P, Plantalech O, Quach J, Resnick AC, Rodenburg SYA, Satravada BA, Schaeffer F, Sheridan R, Singh J, Sirohi R, Sumer SO, van Hagen S, Wang A, Wilson M, Zhang H, Zhu K, Rusk N, Brown S, Lavery JA, Panageas KS, Rudolph JE, LeNoue-Newton ML, Warner JL, Guo X, Hunter-Zinck H, Yu TV, Pilai S, Nichols C, Gardos SM, Philip J; AACR Project GENIE BPC Core Team, AACR Project GENIE Consortium; Kehl KL, Riely GJ, Schrag D, Lee J, Fiandalo MV, Sweeney SM, Pugh TJ, Sander C, Cerami E, Gao J, Schultz N. Analysis and Visualization of Longitudinal Genomic and Clinical Data from the AACR Project GENIE Biopharma Collaborative in cBioPortal. Cancer Res. 2023 Dec 1;83(23):3861-3867. doi: 10.1158/0008-5472.CAN-23-0816. PMID: 37668528; PMCID: PMC10690089.

11. Blum A, Wang P, Zenklusen JC. SnapShot: TCGA-Analyzed Tumors. Cell. 2018 Apr 5;173(2):530. doi: 10.1016/j.cell.2018.03.059. PMID: 29625059.

Let’s work together:

Connect with us at oncology@abcam.com

progress happens together

abcam

danaher